

# Photochemical roles of rapid economic growth and potential abatement strategies on tropospheric ozone over South and East Asia in 2030

S. Chatani<sup>1</sup>, M. Amann<sup>2</sup>, A. Goel<sup>3</sup>, J. Hao<sup>4</sup>, Z. Klimont<sup>2</sup>, A. Kumar<sup>3</sup>, A. Mishra<sup>3</sup>, S. Sharma<sup>3</sup>, S. X. Wang<sup>4</sup>, Y. X. Wang<sup>4</sup> and B. Zhao<sup>4</sup>

[1]{Toyota Central R&D Labs., Inc., Nagakute, Japan}

[2]{International Institute for Applied Systems Analysis, Laxenburg, Austria}

[3]{The Energy and Resources Institute, New Delhi, India}

[4]{Tsinghua University, Beijing, China}

Correspondence to: S. Chatani (schatani@mosk.tytlabs.co.jp)

## Abstract

A regional air quality simulation framework including the Weather Research and Forecasting modelling system (WRF), the Community Multi-scale Air Quality modeling system (CMAQ), and precursor emissions to simulate tropospheric ozone over South and East Asia is introduced. Concentrations of tropospheric ozone and related species simulated by the framework are validated by comparing with observation data of surface monitorings, ozone zondes, and satellites obtained in 2010. The simulation demonstrates acceptable performance on tropospheric ozone over South and East Asia at regional scale. Future energy consumption, carbon dioxide (CO<sub>2</sub>), nitrogen oxides (NO<sub>x</sub>), and volatile organic compound (VOC) emissions in 2030 under three future scenarios are estimated. One of the scenarios assumes a business-as-usual (BAU) pathway, and other two scenarios consider implementation of additional energy and environmental strategies to reduce energy consumption, CO<sub>2</sub>, NO<sub>x</sub>, and VOC emissions in China and India. Future surface ozone under these three scenarios is predicted by the simulation. The simulation indicates future surface ozone significantly increases around India for a whole year and around north eastern China in summer. NO<sub>x</sub> is a main driver on significant seasonal increase of surface ozone, whereas VOC as well as

1 increasing background ozone and methane is also an important factor on annual average of  
2 surface ozone in East Asia. Warmer weather around India is also preferable for significant  
3 increase of surface ozone. Additional energy and environmental strategies assumed in future  
4 scenarios are expected to be effective to reduce future surface ozone over South and East Asia.

5

## 6 **1 Introduction**

7 China, India, and other developing countries in Asia are accomplishing rapid economic  
8 growth. On the other hand, expanding economic activities have caused significant increase of  
9 energy consumption and carbon dioxide (CO<sub>2</sub>) emissions as well as heavy air pollution. One  
10 of key air pollutants is tropospheric ozone. Rising trends of tropospheric ozone have been  
11 observed at least in Japan (Kurokawa et al., 2009; Tanimoto, 2009), China (Xu et al., 2008;  
12 Tang et al., 2009; Wang et al., 2009), and India (Kulkarni et al., 2010). Ozone has adverse  
13 effects on human health (WHO, 2006) and vegetation (Mauzerall and Wang, 2001). In  
14 addition, tropospheric ozone is getting more attentions as one of short-lived climate pollutants  
15 (SLCPs). Reduction of tropospheric ozone may achieve co-benefits which would save human  
16 health and vegetation, and simultaneously mitigate near-term climate change (Shindell et al.,  
17 2012). Tropospheric ozone could be transported across countries as its lifetime in the  
18 atmosphere is relatively long among air pollutants (Akimoto, 2003). Therefore, multilateral  
19 strategies would be desired to reduce tropospheric ozone at regional scale.

20 Ozone is not directly emitted from emission sources. It is formed in the atmosphere from  
21 precursors including nitrogen oxides (NO<sub>x</sub>) and volatile organic compounds (VOCs) via  
22 photochemical reactions. Numerical simulation models which represent photochemical  
23 reactions in the atmosphere are frequently applied to consider how to control precursor  
24 emissions in order to reduce tropospheric ozone. The community of global models has  
25 conducted several studies to predict future tropospheric ozone. For example, the Atmospheric  
26 Chemistry and Climate Model Intercomparison Project (ACCMIP) conducted the  
27 intercomparison of the tropospheric ozone (Young et al., 2013) and its radiative forcing  
28 (Stevenson et al., 2013) in past and future years simulated by the participating global models.  
29 However, there are limitations in these studies. One of them is coarse resolutions applied in  
30 global models. They may not be suitable to simulate tropospheric ozone over densely polluted  
31 regions such as megacities in Asia. Another limitation is future scenarios. Global future  
32 scenarios originally for green house gases (GHGs) are often used in their studies. However,

1 superficial extrapolations of GHGs to air pollutants would lead to misleading conclusions  
2 (Amann et al., 2013). ACCMIP utilized four Representative Concentration Pathways (RCPs)  
3 (Van Vuuren et al., 2011). RCPs have been developed on the basis of emissions and  
4 associated concentrations of greenhouse gases. Although emissions of atmospheric air  
5 pollutants are also estimated in RCPs, Van Vuuren et al. (2011) mentioned that there are  
6 limitations in the use of RCPs for specific air pollution applications because they assumed  
7 that air pollution control becomes more stringent just as a result of rising income levels. That  
8 means they imply an endogenous strengthening of legislation and compliance beyond what is  
9 currently agreed (Amann et al., 2013). Moreover, each RCP has been developed by different  
10 modelling groups. Their assumptions on socioeconomic drivers and climate policies are not  
11 necessarily consistent. Therefore, differences among RCPs cannot be directly interpreted as  
12 effects of specific policies. They are not suitable to consider what, when, and how strategies  
13 should be implemented in individual countries to suppress tropospheric ozone.

14 ~~The purpose of this study is to~~ This paper describes prediction of tropospheric ozone over  
15 South and East Asia in 2030 under future scenarios by using three-dimensional regional air  
16 quality simulations of which the resolution is much finer than global models. Several studies  
17 applied regional air quality simulations in East Asia. For example, Yamaji et al. (2008)  
18 conducted ~~a similar study, but there are some notable differences.~~ simulations to predict future  
19 surface ozone over East Asia. Kurokawa et al. (2009) and Chatani and Sudo (2011) showed  
20 good performances of the simulations to reproduce the trend of surface ozone over Japan for  
21 past years. Although applications in South Asia are limited, Kumar et al. (2012) described  
22 extensive validation of the regional simulations applied over South Asia. One of the  
23 outstanding features of this study is the domain covering China and India together, which are  
24 both key developing countries in Asia. Our target domain covered India, which is one of key  
25 ~~developing countries besides China in Asia.~~ Three future scenarios were developed in this  
26 study. The first scenario assumed a business-as-usual pathway. Future changes in NO<sub>x</sub> and  
27 VOC emissions not only in China but also all the other Asian countries including India were  
28 estimated. The second scenario assumed implementation of additional energy strategies  
29 aiming at reducing energy consumption and CO<sub>2</sub> emissions in China and India. They also  
30 resulted in reduction of NO<sub>x</sub> and VOC emissions. The third scenario assumed implementation  
31 of additional environmental strategies aiming at reducing NO<sub>x</sub> and VOC emissions in China  
32 and India in addition to energy strategies. ~~Simulation results for these future scenarios made~~  
33 ~~possible~~ The purpose of this study is to evaluate effects of potential energy and environmental

1 strategies implemented in China and India on tropospheric ozone over South and East Asia  
2 based on simulated results for three future scenarios. Abatement costs required to implement  
3 these strategies were also estimated. The information regarding to effects and associated  
4 abatement costs of various energy and environmental strategies in China and India obtained in  
5 this study would be helpful to consider effective energy and environmental policies which  
6 should be introduced in both countries to suppress tropospheric ozone as well as energy  
7 consumption and CO<sub>2</sub> emissions. It must be noted that the horizontal resolution of the  
8 regional air quality simulations is 60 km x 60 km. Therefore, it cannot inherently represent a  
9 horizontal variation below 60 km x 60 km. The target of this study is regional tropospheric  
10 ozone above this horizontal scale, which is not directly affected by local sources.

11 Section 2 describes details of the three-dimensional regional air quality simulation  
12 framework organized in this study. Section 3 evaluated model performances on tropospheric  
13 ozone and related species. Section 4 discusses simulated results of future tropospheric ozone.  
14 The outcomes obtained in this study are summarized in Sect. 5. Note that this paper mainly  
15 focuses on air quality simulations. Details of estimating energy consumption, precursor  
16 emissions, and abatement costs are described elsewhere (see Sect. 2.2).

## 18 **2 Simulation setup**

### 19 **2.1 Model configurations**

20 The Community Multi-scale Air Quality modeling system (CMAQ) (Byun and Schere,  
21 2006) version 5.0.1 was applied to simulate concentrations of ambient gaseous and aerosol  
22 species including ozone. Gas-phase chemistry was represented in the Carbon Bond 05  
23 mechanism with updated toluene chemistry (CB05-TU) (Whitten et al., 2010). Aerosol  
24 processes were represented in the AERO6 module. Meteorological inputs were obtained by  
25 running the Weather Research and Forecasting modelling system (WRF) - Advanced  
26 Research WRF (WRF-ARW) (Skamarock et al., 2008) version 3.4.1. The European Centre  
27 for Medium-Range Weather Forecasts (ECMWF) interim reanalyses (ERA-Interim) (Dee et  
28 al., 2011), and the daily, high-resolution, real-time, global, sea surface temperature  
29 (RTG\_SST) analyses compiled by the National Centers for Environmental Prediction (NCEP)  
30 were used for initial and boundary conditions as well as grid nudging in WRF-ARW.

1 The target domains of WRF-ARW and CMAQ are shown in Fig. 1. It covers South, East,  
2 and Southeast Asian countries including Japan in the east, Mongolia in the north, Pakistan in  
3 the west, and Indonesia in the south. The horizontal resolution is 60 km x 60 km. 41 vertical  
4 layers are set from the ground to 5639 Pa above (approximately 19.5 km) in WRF-ARW, and  
5 they are collapsed into 28 layers in CMAQ. The bottom layer height is approximately 34 m in  
6 both models.

7 Boundary concentrations of CMAQ were retrieved from the results of Model for Ozone  
8 and Related chemical Tracers, version 4 (MOZART-4) (Emmons et al., 2010) which was  
9 driven by the meteorological fields simulated by the Goddard Earth Observing System Model,  
10 version 5 (GEOS-5). They were obtained from the National Center for Atmospheric Research  
11 (NCAR, 2013). They were updated every 6 h, and were temporally and spatially interpolated  
12 to the boundaries of the domain.

13 All the simulations discussed in this paper were performed for fourteen months from  
14 November 2009 to December 2010 whereas results for the first month were discarded as a  
15 spin-up period. Future changes in meteorological fields were not considered in this study.

16

## 17 **2.2 Energy and emission data**

18 We estimated energy consumption and emissions of various species including CO<sub>2</sub> in  
19 2010 (referred as BASE) in 22 Asian countries (Bangladesh, Bhutan, Brunei, Cambodia,  
20 China, India, Indonesia, Japan, North Korea, South Korea, Laos, Malaysia, Mongolia,  
21 Myanmar, Nepal, Pakistan, Philipinnes, Singapore, Sri Lanka, Taiwan, Thailand, and  
22 Vietnam). We also developed three future scenarios (BAU0, PC0, and PC1) which were  
23 designed following the concept of Xing et al. (2011) for 2030. BAU0 assumed a business as  
24 usual pathway. The energy and environmental legislations which have been currently  
25 determined were reflected in BAU0. PC0 assumed additional legislations and technological  
26 developments to suppress energy consumption and CO<sub>2</sub> emissions in China and India. PC1  
27 assumed additional legislations and technological developments to improve air quality in  
28 China and India besides PC0. Socioeconomic drivers like population and gross domestic  
29 product (GDP) were consistent in all the scenarios. Differences between BAU0 and PC0, and  
30 PC0 and PC1 correspond to effects of additional energy and environmental strategies  
31 implemented in China and India, respectively. It should be noted that future changes in  
32 emissions of species except for CO<sub>2</sub>, NO<sub>x</sub>, and VOC were not considered in this study. PC0

1 and PC1 considered additional energy and environmental strategies implemented only in  
2 China and India. Energy consumption and emissions in the countries except for China and  
3 India are the same in BAU0, PC0, and PC1. Following subsections briefly introduce them  
4 whereas detailed descriptions of methodologies are found in references shown therein.

5

### 6 **2.2.1 China**

7 The database of anthropogenic energy consumption and emissions in China used in this  
8 study has been originally developed by Wang et al. (2011) and Xing et al. (2011) for current  
9 and future years. This study used the database recently updated by Zhao et al. (2013a, b, c).  
10 Emissions of sulphur dioxide, ammonia, PM<sub>10</sub>, PM<sub>2.5</sub>, black carbon, and organic carbon as  
11 well as CO<sub>2</sub>, NO<sub>x</sub>, and VOC have been estimated for current years. VOC emissions have  
12 been speciated into CB05 species groups (Wei et al., 2008). The horizontal resolution of the  
13 data used in this study is 36 km x 36 km.

14 The annual energy consumption and CO<sub>2</sub>, NO<sub>x</sub>, and VOC emissions estimated for 2010  
15 (BASE) and 2030 under the three future scenarios in China are shown in Table 1. The  
16 VOC/NO<sub>x</sub> emission ratios are also shown. The energy consumption increases by 64% from  
17 BASE to BAU0 due to growing economic activities. The CO<sub>2</sub> emissions increase in similar  
18 magnitude by 66%. Increases of the NO<sub>x</sub> and VOC emissions are 35% and 27%, which are  
19 relatively lower than that of energy consumption. Current environmental legislations  
20 effectively reduce NO<sub>x</sub> and VOC emissions per energy consumption. The additional energy  
21 strategies assumed in PC0 realizes 22%, 30%, 29%, and 16% decreases of the energy  
22 consumption and CO<sub>2</sub>, NO<sub>x</sub>, and VOC emissions, respectively. They make the NO<sub>x</sub> and  
23 VOC emissions comparable to those in BASE. The additional environmental strategies  
24 assumed in PC1 further reduce the NO<sub>x</sub> and VOC emissions by 55% and 31%, which become  
25 significantly lower than those in BASE. The VOC/NO<sub>x</sub> ratio increases from 0.82 in BAU0 to  
26 1.47 in PC1 as NO<sub>x</sub> is more effectively reduced than VOC by the assumed energy and  
27 environmental strategies.

28

## 1 **2.2.2 India**

2 The database of anthropogenic energy consumption and emissions in India used in this  
3 study has been developed by Sharma et al. (2014). Emissions of carbon monoxide, sulphur  
4 dioxide, and total suspended particulates (TSP) as well as CO<sub>2</sub>, NO<sub>x</sub>, and VOC have been  
5 estimated for current years. VOC emissions have been speciated into CB05 species groups.  
6 The horizontal resolution of the data used in this study is 36 km x 36 km.

7 The annual energy consumption and emissions estimated for 2010 (BASE) and 2030  
8 under the three future scenarios in India are shown in Table 1. The energy consumption and  
9 CO<sub>2</sub> emissions dramatically increase by 3.2 and 2.9 times from BASE to BAU0 due to rapid  
10 economic growth assumed in the scenarios (8% per year). The NO<sub>x</sub> emissions also  
11 significantly increase by 3.5 times. Although legislations to reduce NO<sub>x</sub> emissions have been  
12 already implemented, growing economy increases dependence on coal power plants, heavy  
13 industries, and vehicles, of which NO<sub>x</sub> emissions per energy consumption is relatively high.  
14 On the other hand, magnitude of increase of the VOC emissions is below twice. The assumed  
15 decrease of dependence on biomass fuel in domestic use, which is the dominant VOC  
16 emission source in BASE, suppresses increase of VOC emissions. That also results in  
17 significant changes of the VOC/NO<sub>x</sub> ratios. It is 1.82 in BASE, which is much higher than  
18 China, and decreases to 1.02 in BAU0. The additional energy strategies assumed in PC0  
19 realizes 26%, 32%, 31%, and 20% decreases of the energy consumption and CO<sub>2</sub>, NO<sub>x</sub>, and  
20 VOC emissions, respectively. The additional environmental strategies assumed in PC1 further  
21 reduce the NO<sub>x</sub> and VOC emissions by 49% and 29%, which become comparable to those in  
22 BASE. The VOC/NO<sub>x</sub> ratio increases to 1.68 in PC1 as NO<sub>x</sub> is effectively reduced than VOC  
23 by energy and environmental strategies as in the case of China.

24

## 25 **2.2.3 Other Asian countries**

26 The data of anthropogenic energy consumption and emissions in other Asian countries  
27 than China and India were obtained from the results of the Greenhouse Gas and Air Pollution  
28 Interactions and Synergies (GAINS)-Asia model (Klimont et al., 2009; Amann et al., 2011)  
29 under World Energy Outlook 2011 (IEA, 2011) energy projections. GAINS-Asia has a  
30 capability to estimate energy consumption and emissions in 99 regions in Asia. In addition,  
31 the gridded data of which the horizontal resolution is 0.5 degree x 0.5 degree are also

1 available (IIASA, 2013). The results of GAINS-Asia model for 99 regions were used to  
2 develop speciation factors for each sector, fuel and region based on SPECIATE 4.3 (USEPA,  
3 2013) because the detailed information of sectors and fuels are available. Then, they were  
4 applied to the gridded data to convert VOC emissions into CB05 species groups.

5 The annual energy consumption and emissions estimated for 2010 (BASE) and 2030  
6 (BAU0) in major Asian countries (Japan, South Korea, Thailand, and Indonesia) are shown in  
7 Table 1. Japan and South Korea indicate a different pathway from Thailand and Indonesia.  
8 The energy consumption and CO<sub>2</sub> emissions are comparable for BASE and BAU0 in Japan  
9 and South Korea. The NO<sub>x</sub> and VOC emissions in BAU0 are lower than BASE in both  
10 countries. On the other hand, energy consumption and emissions of CO<sub>2</sub> and NO<sub>x</sub>  
11 significantly increase from BASE to BAU0 in Thailand and Indonesia. Decrease of the VOC  
12 emissions in Thailand and Indonesia in BAU0 is mainly due to decrease of 2-wheel  
13 motorcycles in vehicles fleets.

14

#### 15 **2.2.4 Other emissions**

16 Monthly values in the Global Fire Emissions Database (GFED) (Van der Werf et al.,  
17 2010) version 3.1 were applied for biomass burning emissions. Emissions from agricultural  
18 burning in GFED were ignored because they are included in the anthropogenic emissions  
19 described in previous subsections. Emission Database for Global Atmospheric Research  
20 (EDGAR) version 4.1 (European Commission, 2010) was applied for international shipping  
21 emissions. Hourly biogenic emissions were estimated by the Model of Emissions of Gases  
22 and Aerosols from Nature (MEGAN) (Guenther et al., 2006) version 2.04. Future changes in  
23 these emissions were not considered in this study.

24

### 25 **3 Model performance**

26 A simulation for the case using emissions for 2010 (BASE) was performed. Horizontal  
27 distributions of the simulated seasonal mean surface ozone concentration are shown in Fig. 2a.  
28 Note that averaged values of daily 8 h maximum ozone concentration within the bottom 3  
29 layers (approximately 134 m) are discussed as mean surface ozone concentration hereafter in  
30 this paper because they are the most relevant to consider adverse effects on human health and  
31 vegetation. Notable seasonal features are found in horizontal distributions. A zone with high

1 concentration encompasses mid-latitude regions from India to Japan in spring and autumn. It  
2 is shifted northward and the highest concentration appears around north eastern China in  
3 summer. By the contrary, the concentration significantly decreases around the same region in  
4 winter. The concentration is low for a whole year around the equator while some hot spots are  
5 found around megacities. Excited oxygen atoms, which are dissociated from ozone, are likely  
6 to be scavenged by abundant water vapour instead of reproducing ozone.

7 The simulated results of ozone and related species were compared with observations to  
8 validate them as discussed in following subsections. Although it should be avoided to use the  
9 observation data directly affected by local sources, some data had to be included due to  
10 limited data availability in the target region. We additionally relied on the satellite data. Its  
11 great advantage is comparisons between observed and simulated values which are both  
12 consistently averaged in the same individual meshes. It is suitable to validate the regional air  
13 quality simulations in this study.

### 15 3.1 Surface ozone

16 Surface ozone concentration is continuously observed at the Acid Deposition Monitoring  
17 Network in East Asia (EANET) monitoring sites. It is an ideal monitoring network to validate  
18 the simulations in this study because the monitoring sites are mainly located in remote areas.  
19 ~~The monthly mean surface ozone concentration observed at the ten EANET~~ monitoring sites  
20 ~~which are~~ classified as “Rural” and “Remote” were picked up to avoid sites affected by local  
21 sources (Network Center for EANET, 2012). The monthly mean surface ozone concentration  
22 observed at these sites and the corresponding values simulated in the bottom layer are  
23 compared as shown in Fig. 3. The results of MOZART-4 in its bottom layer are also shown in  
24 it. The locations of the twelve EANET monitoring sites are indicated in Fig. 1. Most of them  
25 are located in Japan and South Korea.

26 The observed values are high in spring and low in summer. Peak values and seasonal  
27 variations are reasonably reproduced by the simulation. One of the problems is that the low  
28 values observed in summer are overestimated in the simulation at several sites. Such a  
29 tendency is more evident in the results of MOZART-4. The simulation in this study makes  
30 effectively the simulated values closer to the observed ones as realized at Rishiri and Ochiishi.  
31 However, declines of the observed values in summer are still not fully reproduced at Sado-  
32 seki, Oki, Cheju, and Imsil, which are located in or around Japan Sea. It appears that the

1 simulation in this study and MOZART-4 share common difficulties in reproducing low values  
2 around Japan Sea in summer. Southerly winds are dominant but westerly winds also appear  
3 for some days in summer around Japan and South Korea. Relationships between the hourly  
4 surface ozone and wind direction at Sado-seki and Oki were investigated (not shown). It  
5 turned out that westerly winds mainly cause overestimation at both sites. The simulated  
6 values are the highest around upwind regions of westerly winds in summer as shown in Fig.  
7 2a. Lin et al. (2009) and Chatani and Sudo (2011) have showed that surface ozone was  
8 overestimated around corresponding regions in their simulations. Excess ozone may be  
9 transported downwind to South Korea and Japan on westerly winds and cause overestimation  
10 in this study, too. Lin et al. (2009) implied surface ozone is highly sensitive to cloud cover  
11 and monsoonal rainfall over these regions. Chatani and Sudo (2011) mentioned uncertainties  
12 in emission inventory and coarse resolution as well as potential missing pathways in the  
13 chemical mechanisms embedded in the model as possible reasons for overestimation. The  
14 simulation in this study as well as MOZART-4 may still have similar difficulties in accurately  
15 representing these factors.

16 There is no monitoring network similar to EANET in South Asia. Kumar et al. (2012)  
17 validated their simulation by comparing the simulated monthly mean values of surface ozone  
18 with the observed data at the seven sites in India which had been published in the past  
19 literatures. The target years of the observed data were not necessarily consistent with their  
20 simulation. We follow Kumar et al. (2012), though a part of the data is substituted with the  
21 data published in more recent literatures. As a result, the observed data of surface ozone at  
22 Ahmedabad (Lal et al., 2000), Gadanki (Naja and Lal, 2002), Mt. Abu (Naja et al., 2003),  
23 Pune (Beig et al., 2007), Anantapur (Reddy et al., 2012), Nainital (Kumar et al., 2010), and  
24 Thumba (David and Nair, 2011) were picked up in this study. The locations of these seven  
25 sites are indicated in Fig. 1. Some of them are not located in remote areas. The monthly mean  
26 surface ozone concentration observed at them and the corresponding values simulated in the  
27 bottom layer are compared as shown in Fig. 4. The results of MOZART-4 in its bottom layer  
28 are also shown in it.

29 The observed values are high in late winter or spring, and low in summer. Such seasonal  
30 variations are generally reproduced in most sites including Anantapur, where the target year  
31 of the observed values is coincident with the simulation. The model performance at all the  
32 sites is comparable to Kumar et al. (2012). One of notable differences from them is

1 amplitudes of seasonal variations. Kumar et al. (2012) showed better performance on low  
2 values in summer, though peak values in winter were significantly overestimated. The  
3 performance of the simulation in this study is opposite with them. Peak values in winter are  
4 reasonably reproduced whereas low values in summer is slightly overestimated. The reason is  
5 probably due to seasonal variations in emissions. Information regarding to seasonal variations  
6 in emissions in India have not been available in the database described in Sect. 2.2.2, whereas  
7 Kumar et al. (2012) applied seasonal variations represented in the Reanalysis of Tropospheric  
8 Chemical Composition (RETRO) database. The model performance in this study could be  
9 improved if any seasonal variations in emissions are applied. In addition, the total amount of  
10 NO<sub>x</sub> emissions developed in this study for India is less than the Intercontinental Chemical  
11 Transport Experiment - Phase B (INTEX-B) inventory (Zhang et al., 2009) which was used in  
12 Kumar et al. (2012). It may prevent significant overestimation of surface ozone in winter in  
13 this study.

14 The surface ozone is overestimated in Ahmedabad and Thumba throughout the year. The  
15 station in Ahmedabad is located in the urban area (Lal et al., 2000). The station in Thumba is  
16 located 10 km away from the city center (David and Nair, 2011). It appears that the observed  
17 values at the both stations are affected by local sources. MOZART-4 also overestimates the  
18 values at the both stations, implying a limitation to reproduce low values with the current  
19 horizontal resolution. Simulated ozone around local sources is influenced by a horizontal  
20 resolution, and its temporal mean values tend to become lower with higher resolution  
21 (Chatani et al, 2011). Such a low value affected by local sources is not the target of this study.

22

### 23 **3.2 Vertical ozone profile**

24 Vertical concentration profiles of the simulated ozone were compared with those of the  
25 ozone observed by ozonesonde at three stations (Sapporo, Tsukuba, and Naha) in Japan (JMA,  
26 2012), one station in Hong Kong (Hong Kong Observatory, 2012), and two stations (Delhi  
27 and Thiruvananthapuram) in India (India Meteorological Department, 2013) which are  
28 archived by World Ozone and Ultraviolet Radiation Data Centre (WOUDC). The locations of  
29 the six stations are shown in Fig. 1. Vertical profiles of the observed and simulated values at  
30 them are compared as shown in Fig. 5. Measurements have been conducted several times in  
31 each season at Sapporo, Tsukuba, Naha, and Hong Kong. Both of the observed and simulated  
32 values at these four stations are those averaged over all the measurements conducted within

1 each season. On the other hand, any values observed at Delhi and Thiruvananthapuram in  
2 2010 are not available. Therefore, the simulated seasonal mean values are compared with the  
3 observed values averaged over all the available measurements in each season during 2000-  
4 2011 in Fig. 5 following Kumar et al. (2012). High gradients of the values observed in the  
5 upper troposphere are well reproduced by the simulation. The older versions of CMAQ had a  
6 problem in simulating them adequately when results of global scale models were utilized as  
7 boundary concentrations (Lam and Fu, 2009). The latest version of CMAQ used in this study  
8 has updated the representation of turbulent mixing during stable conditions and updates to the  
9 vertical advection scheme to reduce numerical diffusion in the upper model layers. It appears  
10 this update has contributed to significant improvement of the performance on vertical profile.  
11 The profiles in the lower and middle troposphere are also well reproduced, but the simulated  
12 values tend to be slightly higher around the surface and lower in the middle troposphere than  
13 the observed values except for Thiruvananthapuram. The simulated values are almost constant  
14 from the surface up to 200 hPa whereas a weak gradient are found in the values observed at  
15 Thiruvananthapuram. Uncertainties in vertical diffusions may result in deviations between the  
16 observed and simulated values, and cause excessive accumulation of ozone in summer in the  
17 lower layers of the simulation shown in Figs. 3 and 4.

18

### 19 **3.3 Tropospheric column NO<sub>2</sub>**

20 Tropospheric column NO<sub>2</sub>, which is one of major precursors of ozone, has been retrieved  
21 from the observations of the Ozone Monitoring Instrument (OMI) mounted on the Earth  
22 Observing System (EOS) Aura satellite. The second release of collection 3 OMI/Aura Level-2  
23 NO<sub>2</sub> data product OMNO2 (Bucsela et al., 2013) available at the National Aeronautics and  
24 Space Administration (NASA) Goddard Earth Sciences Data and Information Services Center  
25 (2012) was used in this study. The retrieved data of tropospheric column NO<sub>2</sub> within the  
26 target domain without any problems were selected based on their quality flags. The  
27 corresponding simulated value at the same location and timing were also picked up. Horizontal  
28 distributions of their seasonal mean values are shown in Fig. 6. The observed and simulated  
29 monthly mean values averaged over the regions shown in Fig. 1 in China and India as well as  
30 other major countries (Japan, South Korea, Thailand, and Indonesia) are shown in Fig. S1 in  
31 the Supplement.

1 The observed values are high around populated regions including North China Plain  
2 (Huabei), Yangtze River Delta (Huadong), Pearl River Delta (Huanan), Seoul (South Korea),  
3 and Tokyo (Japan) in East Asia. They indicate a clear seasonal variation with high values in  
4 winter and low values in summer. These features are well reproduced by the simulation as  
5 shown by Wang et al. (2011) which used the consistent emissions with this study. The values  
6 are systematically lower in South and Southeast Asia because NO<sub>x</sub> emissions are significantly  
7 lower than East Asia. Note that the ranges of tropospheric column NO<sub>2</sub> in Fig. S1 in the  
8 Supplement are different in East and South/Southeast Asia. The values are underestimated by  
9 the simulation except for summer in South and Southeast Asia. As discussed in Sect. 3.1,  
10 possible reasons of underestimated NO<sub>2</sub> are the total amount and seasonal variation of NO<sub>x</sub>  
11 emissions developed in this study. Ghude et al. (2013) derived 1.9 TgN year<sup>-1</sup> as the  
12 optimized total amount of NO<sub>x</sub> emissions for India in 2005 by using an inverse technique and  
13 iterative procedure to minimize gaps between their simulated values and the observed values  
14 derived from OMI. The total amount of NO<sub>x</sub> emissions developed in this study for India  
15 discussed in Sect. 2.2.2 is equivalent to 1.7 TgN year<sup>-1</sup>. If economic growth during 2005-2010  
16 is taken into account, the NO<sub>x</sub> emissions developed in this study seems to be underestimated.  
17 Kumar et al. (2012) showed their simulation overestimated tropospheric column NO<sub>2</sub> over  
18 Indo-Gangetic Plain (Center) in winter, and underestimated it in rest of seasons and regions.  
19 Such a spatial difference in the performance is not found in this study. The horizontal  
20 distribution of the NO<sub>x</sub> emissions developed in this study may prevent accumulating NO<sub>x</sub> in  
21 Indo-Gangetic Plain.

22

### 23 **3.4 Total column CO**

24 CO is also an important precursor of ozone as well as a product in photochemical  
25 reactions involving VOCs. Therefore, validations for CO are valuable in terms of ozone  
26 formation and VOC emissions. Total column CO has been retrieved from the observations of  
27 the Measurements Of Pollution In The Troposphere (MOPITT) mounted on the Earth  
28 Observing System (EOS) Terra satellite. The MOPITT Version 4 (Deeter et al., 2010) Level 2  
29 product was used in this study. The retrieved data of total column CO within the target  
30 domain without any problems were selected based on their quality flags. The corresponding  
31 simulated value at the same location and timing were also picked up. Horizontal distributions

1 of their seasonal mean values are shown in Fig. 7. The observed and simulated monthly mean  
2 values averaged over the regions are shown in Fig. S2 in the Supplement.

3 The observed values are high from winter to spring in east China, Indochina peninsula,  
4 and India. The values in Indochina peninsula and India become much lower in summer and  
5 autumn. Such a seasonal variation is well reproduced by the simulation, though the higher  
6 values from winter to spring are slightly underestimated in this study. Biomass burning is  
7 active in the corresponding regions and the seasons in which the observed values are high. It  
8 implies that the GFED biomass burning emissions used in this study are underestimated.  
9 Pechony et al. (2013) also indicated that the GFED emissions are significantly underestimated  
10 in South and Southeast Asia in their inverse modelling using MOPITT and Tropospheric  
11 Emission Spectrometer (TES) satellite data.

12

### 13 **3.5 Tropospheric column ozone**

14 Ziemke et al. (2006) has derived tropospheric column ozone by subtracting stratospheric  
15 column ozone observed by Microwave Limb Sounder (MLS) mounted on EOS from total  
16 column ozone observed by OMI. The data of their monthly mean tropospheric column ozone  
17 was obtained from the NASA Goddard Space Flight Center (2012). Horizontal distributions of  
18 their seasonal mean values are shown in Fig. 8. The simulated values at the locations and  
19 timings from the surface up to the tropopause at which total column ozone was retrieved by  
20 OMI without any problems were picked up based on quality flags of the version 3 of the  
21 OMI/Aura Ozone Total Column Level-2 data product (OMTO3). The tropopause was  
22 determined as the height at which a gradient of temperature becomes lower than  $2 \text{ K km}^{-1}$  in  
23 the values simulated by WRF (Kumar et al., 2012) above 316 hPa, which is the lowest  
24 altitude retrieved from MLS. Horizontal distributions of their seasonal mean values are also  
25 shown in Fig. 8. The observed and simulated monthly mean values averaged over the regions  
26 are shown in Fig. S3 in the Supplement.

27 The observed values are high over the mid latitude in spring. The zone with high values  
28 is shifted northward in summer, and causes elevated values over northeast China. Such  
29 features in horizontal distribution are well reproduced in the simulation. The observed values  
30 are highest in summer in most of East Asia as shown in Fig. S3 in the Supplement whereas  
31 surface ozone shown in Fig. 3 in corresponding regions is lowest in summer. The observed  
32 and simulated values in all months agree well in Huabei where surface ozone is highest in

1 summer. Therefore, uncertainties in vertical profiles of ozone shown in Fig. 5 may be a major  
2 factor causing overestimation of surface ozone in East Asia as discussed in Sect. 3.3. The  
3 simulated values are higher than the observed ones over the mid latitude in winter. The  
4 difference between observed and simulated monthly column ozone is 12 DU (37.9%) in  
5 January in Center (India), and the difference between observed and simulated seasonal  
6 column ozone is 8.0 DU (24%) in DJF in the same region at the maximum. Ziemke et al.  
7 (2006) showed that the column ozone simulated by Global Modeling Initiative's (GMI)  
8 Combined Stratosphere-Troposphere Chemical Transport Model (COMBO CTM) is 5-10 DU  
9 higher than the value obtained from OMI/MLS in DJF in the corresponding region. The  
10 model performance in this study is comparable to them.

11 Although some issues which should be solved to improve the model performance on  
12 ozone still remain, we have judged the regional air quality simulation framework constructed  
13 in this study has acceptable performance to predict tropospheric ozone at regional scale based  
14 on validations described in this section.

#### 16 **4 Future prediction**

17 Simulations for the nine cases shown in Table 2 were performed to examine various  
18 factors on surface ozone in 2030. Future changes of surface ozone from 2010 to 2030 were  
19 evaluated in BASE and BAU0 cases. Only NO<sub>x</sub> and VOC emissions were changed from  
20 BASE to BAU0 in BAU0nox and BAU0voc cases, respectively, to evaluate their effects  
21 separately. Boundary ozone concentration was homogeneously increased by 5 ppb in  
22 BAU0o3 to evaluate potential effects of increasing background ozone on tropospheric ozone  
23 within the target domain. Similarly, homogeneous methane concentration was increased by  
24 400 ppb from the value used in the default CMAQ (1850 ppb) in BAU0ch4 to evaluate  
25 potential effects of increasing background methane. The ranges of increasing background  
26 ozone and methane were set based on the maximum changes predicted by Dentener et al.  
27 (2006). Temperature was homogeneously decreased by 5 degree C in BAU0ta to see  
28 sensitivities of temperature on surface ozone. Effects of the additional energy and  
29 environmental strategies on surface ozone in 2030 were evaluated in PC0 and PC1.

#### 1 **4.1 Future surface ozone in the BAU scenario**

2 Horizontal distributions of the seasonal mean surface ozone concentration simulated in  
3 BASE and BAU0 are shown in Fig. 2a and b, respectively. Significant increase of surface  
4 ozone around India in BAU0 is evident in all seasons. Dentener et al. (2006) also indicated  
5 significant increase of future ozone around India under their current legislation (CLE)  
6 scenario. Surface ozone around north eastern China in BAU0 is similarly higher in summer  
7 whereas it is slightly lower in winter than BASE.

8 Horizontal distributions of differences in the simulated seasonal mean surface ozone  
9 concentrations between BAU0nox and BASE, BAU0voc and BASE, and BAU0 and BASE  
10 are shown in Fig. 9. Increase of surface ozone around India and surrounding regions including  
11 south western China and Indochina in all seasons is exclusively affected by increasing NOx.  
12 The effects of VOC are negligible or slightly negative around those regions. Increase of  
13 surface ozone over most of China in summer is also much affected by increasing NOx except  
14 for megacities like Yangtze River Delta and Pearl River Delta while its magnitude is less than  
15 India. Ozone chemistry in India for whole year and China in summer seems to be in NOx-  
16 sensitive regime (Sillman, 1999). Kumar et al. (2012) also implied that the ozone chemistry  
17 over India is NOx-limited except for a part of Indo-Gangetic Plain in winter. On the other  
18 hand, negative effects of increasing NOx appear around north eastern China in spring and  
19 autumn, and they expand to whole eastern China in winter. Increasing VOC has positive  
20 effects around the corresponding regions. Ozone chemistry in eastern China in winter seems  
21 to be in VOC-sensitive regime. Liu et al. (2010) indicated that ozone chemistry in eastern  
22 China is in VOC-sensitive regime in January and NOx-sensitive regime in July. They also  
23 indicated that it is in NOx-sensitive regime in central and western China and in VOC-  
24 sensitive regime in major Chinese megacities throughout the year. Itahashi et al. (2013)  
25 suggested that regime of ozone chemistry in East Asia is NOx-sensitive in summer, VOC-  
26 sensitive in winter, and either NOx- or VOC-sensitive during spring and autumn. The results  
27 obtained in this study are consistent with their findings. Factors that affect NOx- and VOC-  
28 sensitive regimes include VOC/NOx ratios as well as meteorological conditions (Sillman,  
29 1999). Table 1 shows VOC/NOx ratios in BASE are much higher in India than China. They  
30 may result in stronger sensitivities of NOx around India. Effects of NOx are negative in all  
31 seasons, and those of VOC are also negative in summer around Japan and South Korea.

1 Although a part of them may be affected by transport from China, decrease of domestic NO<sub>x</sub>  
2 and VOC emissions should contribute to decrease of surface ozone around this region.

3

#### 4 **4.2 Effects of external factors on future surface ozone**

5 Horizontal distributions of differences in the simulated seasonal mean surface ozone  
6 concentrations between BAU0o<sub>3</sub> and BAU0, and BAU0ch<sub>4</sub> and BAU0 are shown in Fig. 10.  
7 The effect of boundary ozone is reduced around regions where a lot of chemical species are  
8 emitted and react with ozone. Decrease of the effect is more evident in summer due to more  
9 active photochemical reactions. The effect is also lower around tropical regions with abundant  
10 water vapour. Nevertheless, increasing boundary ozone may cause a few ppb increase of  
11 surface ozone throughout the domain especially in winter over mid-latitude regions as  
12 discussed by Chatani and Sudo (2011). By contrast, the effect of background methane  
13 increases around regions where a lot of chemical species are emitted. Products from methane  
14 in photochemical reactions contribute to net increase of ozone originating in NO<sub>x</sub>. However,  
15 magnitude of the effect of background methane is only a few ppb at a maximum against a  
16 large increase of background methane +400 ppb. It is compensated with effect of boundary  
17 ozone, and combined effects of boundary ozone and background methane do not exceed 5  
18 ppb. Note that the relatively small effect of increasing background methane do not deny its  
19 importance on surface ozone described by Dentener et al. (2005) and Fiore et al. (2008).  
20 Increasing background methane causes a part of increase of background ozone. The effect of  
21 boundary ozone evaluated in this section is partly affected by background methane.

22 Horizontal distributions of differences in the simulated seasonal mean surface ozone  
23 concentrations between BAU0ta and BAU0 are shown in Fig. 11. Negative effect of  
24 decreased temperature is found around regions where surface ozone is abundant such as India  
25 for whole year and north eastern China in summer. The motivation to conduct this sensitivity  
26 analysis is to investigate reasons why surface ozone significantly increases around India for  
27 whole year while it decreases around China in winter even if NO<sub>x</sub> emissions are increased in  
28 both countries in BAU0. It turns out that higher temperature is one of factors which cause  
29 higher ozone concentration. The weather condition around India is warm throughout the year.  
30 Therefore, increase of precursor emissions has larger importance in terms of ozone formation  
31 in India.

32

### 4.3 Effects of energy and environmental strategies on future surface ozone

Horizontal distributions of the seasonal mean surface ozone concentration simulated in PC1 are shown in Fig. 2c. Surface ozone concentration in PC1 is comparable or slightly lower than BASE. Horizontal distributions of differences in the simulated seasonal mean surface ozone concentrations between PC0 and BAU0 and PC1 and BAU0 are shown in Fig. 12. Surface ozone is effectively reduced by the additional energy and environmental strategies around the regions in which it significantly increases from BASE to BAU0. Though, the regions with increasing ozone are found around eastern China where ozone chemistry is in VOC-sensitive regime. They do not mean that energy and environmental strategies are not preferable to mitigate air pollution. Ozone isopleths against NO<sub>x</sub> and VOC have non-linear shapes (Sillman, 1999). If NO<sub>x</sub> is reduced in VOC-sensitive regime, ozone should increase until it goes into NO<sub>x</sub>-sensitive regime. It is essential to reduce NO<sub>x</sub> to pass over the ridge which divides VOC- and NO<sub>x</sub>-sensitive regimes and go into NO<sub>x</sub>-sensitive regime where ozone is effectively reduced. As shown in Fig. 12, the regions with increasing ozone are shrunk in spring and autumn. They imply that regime of ozone chemistry changes from VOC-sensitive to NO<sub>x</sub>-sensitive as VOC/NO<sub>x</sub> ratios increase due to more effective reduction of NO<sub>x</sub> than VOC as shown in Table 1. However, it is difficult to reduce ozone in winter around eastern China. In fact, surface ozone is lower than surrounding regions as shown in Fig. 2b because titration by NO<sub>x</sub> overwhelms ozone formation. Reduction of NO<sub>x</sub> brings surface ozone back to its background level. Nonetheless, it is still necessary to reduce NO<sub>x</sub> because it products like NO<sub>2</sub> and nitrate are also important air pollutants.

### 4.4 Regional summary

Figure 13 shows differences in the simulated monthly mean surface ozone concentrations among cases which are averaged over regions shown in Fig. 1 in China and India as well as other major countries (Japan, South Korea, Thailand, and Indonesia). As discussed in previous sections, different characteristics are found in eastern (Huabei, Dongbei, Huadong, and Huanan) and western (Xinan and Xibei) China. Surface ozone increases from BASE to BAU0, and is effectively reduced in PC0 and PC1 for whole year in western China as well as in India. Although similar responses are found in eastern China in summer, increase of NO<sub>x</sub> from BASE to BAU0 results in decrease of surface ozone in winter. The additional energy and environmental strategies implemented in China and India assumed in PC0 and PC1 are

1 effective to reduce surface ozone even in South Korea and Japan in summer. Decreasing  
2 domestic NO<sub>x</sub> in BAU0 also contributes to decrease of surface ozone in summer in Japan.  
3 Whereas the difference between BAU0voc and BASE is negligible in India, BAU0-BASE\*  
4 (the difference between BAU0 and BASE in which the difference between BAU0nox and  
5 BASE and the difference between BAU0voc and BASE are excluded) is evident. It means  
6 that sum of the individual effects of increasing NO<sub>x</sub> and increasing VOC does not coincident  
7 with the combined effects of increasing NO<sub>x</sub> and VOC. It implies that VOC has some effects  
8 on surface ozone in BAU0 in which the VOC/NO<sub>x</sub> ratio is significantly lowered than BASE.  
9 The additional energy and environmental strategies implemented in India and China assumed  
10 in PC0 and PC1 are effective to reduce surface ozone in late autumn in Thailand where  
11 surface ozone increases due to increasing NO<sub>x</sub> in BAU0. Changes of surface ozone are  
12 negligible in Indonesia while the situation may be different around megacities locally.

13 Figure 14 shows the differences in the simulated annual mean surface ozone  
14 concentrations among cases which are averaged over regions in China and India as well as  
15 other major countries. Note that the ranges of vertical axis are different in East Asia (left) and  
16 South and Southeast Asia (right). The response in each case is simple and consistent with  
17 monthly concentrations in South and Southeast Asia. The increase of annual surface ozone  
18 reaches 20 ppb in Indian regions. Fiore et al. (2012) showed that past model studies predicted  
19 10-15 ppb increase of surface ozone in South Asia during 2000-2030 in the Special Report on  
20 Emission Scenarios (SRES) A2 scenario. NO<sub>x</sub> emission in India becomes twice for  
21 corresponding years in this scenario. This study predicted much larger increase of NO<sub>x</sub>  
22 emission in India as shown in Table 1. Therefore, the significant increase of surface ozone  
23 predicted in this study appears to be consistent in the past model studies shown in Fiore et al.  
24 (2012). On the other hand, the response of annual surface ozone is much complex in East Asia.  
25 The effects of increasing NO<sub>x</sub> in BAU0 in summer and winter are cancelled out in eastern  
26 China, and the effects of increasing VOC are larger. The small effects of PC0 in eastern China  
27 are also due to its opposite effects in summer and winter. In addition, relative importance of  
28 background ozone and methane is also larger in East Asia. Overall and well-designed  
29 strategies are required to effectively reduce annual mean surface ozone in East Asia.

30

## 1 **5 Conclusions**

2 This study constructed a regional air quality simulation framework to simulate  
3 tropospheric ozone over South and East Asia where developing countries are accomplishing  
4 rapid economic growth. It demonstrated acceptable performance on tropospheric ozone at  
5 regional scale while overestimation of low concentration in summer is one of remaining  
6 issues which other simulation studies are also facing. It is necessary to find out a reason and  
7 solve it.

8 The simulations predicted significant increase of surface ozone around India in BAU0.  
9 Increasing NO<sub>x</sub> due to expanding economic activities was a major cause, and warmer weather  
10 contributed to it. Surface ozone was predicted to increase also around north eastern China in  
11 summer due to increasing NO<sub>x</sub> in BAU0. The additional energy and environmental strategies  
12 assumed in PC0 and PC1 are expected to effectively reduce surface ozone in the seasons and  
13 regions in which surface ozone is significantly increased in BAU0. The situation is a bit  
14 complex for annual mean surface ozone in East Asia. Increasing VOC as well as increasing  
15 background ozone and methane are also important for it. Various energy and environmental  
16 strategies are assumed in PC0 and PC1. It is desired to implement them in order of increasing  
17 abatement cost to suppress tropospheric ozone not only in China and India but also  
18 surrounding regions. Energy strategies assumed in PC0 could simultaneously suppress energy  
19 consumption and CO<sub>2</sub> emissions.

20 This study predicted potential future changes of tropospheric ozone due to changes in  
21 precursor emissions in the same meteorological field. It is desirable to check if the trend of  
22 tropospheric ozone for coming years is following the changes simulated in this study to  
23 evaluate the effects of existing strategies in the real atmosphere and to consider additional  
24 strategies. Long-term continuous monitoring of pollutant concentrations, periodical update of  
25 the emission inventory, and simulations for multiple coming years would be helpful.

26 The simulation framework constructed in this study can be applied to not only  
27 tropospheric ozone but also other air quality issues like acid rain and haze. Especially, air  
28 pollution by particulate matter is also one of major environmental issues in Asia. Ambient  
29 particulate matter includes various primary and secondary components. Although this study  
30 estimated future NO<sub>x</sub> and VOC emissions, it is necessary to estimate emissions of other  
31 components and precursors to predict future concentrations of particulate matter. In addition,  
32 strategies implemented in other Asian countries than China and India should affect the air

1 quality over Asia whereas this study mainly focused on China and India. Future energy and  
2 emission scenarios in each country are required to evaluate their effects. We hope the  
3 outcome of this study will contribute to mitigate energy and environmental issues in Asia as a  
4 basis for considering desirable future pathways.

5

## 6 **Acknowledgements**

7 This study was financially supported by Toyota Motor Corporation.

8

## 1 **References**

- 2 Akimoto, H.: Global air quality and pollution, *Science*, 302, 1716-1719,  
3 doi:10.1126/science.1092666, 2003.
- 4 Amann, M., Bertok, I., Borken-Kleefeld, J., Cofala, J., Heyes, C., Höglund-Isaksson, L.,  
5 Klimont, Z., Nguyen, B., Posch, M., Rafaj, P., Sandler, R., Schöpp, W., Wagner, F., and  
6 Winiwarter, W.: Cost-effective control of air quality and greenhouse gases in Europe:  
7 modeling and policy applications, *Environ. Modell. Softw.*, 26, 1489-1501,  
8 doi:10.1016/j.envsoft.2011.07.012, 2011.
- 9 Amann, M., Klimont, Z., and Wagner, F.: Regional and global emissions of air pollutants:  
10 recent trends and future scenarios, *Annu. Rev. Env. Resour.*, 38, 7.1-7.25,  
11 doi:10.1146/annurev-environ-052912-173303, 2013.
- 12 Beig, G., Gunthe, S., and Jadhav, D. B.: Simultaneous measurements of ozone and its  
13 precursors on a diurnal scale at a semi urban site in India, *J. Atmos. Chem.*, 57, 239-253,  
14 doi:10.1007/s10874-007-9068-8, 2007.
- 15 Bucseła, E. J., Krotkov, N. A., Celarier, E. A., Lamsal, L. N., Swartz, W. H., Bhartia, P. K.,  
16 Boersma, K. F., Veefkind, J. P., Gleason, J. F., and Pickering, K. E.: A new stratospheric  
17 and tropospheric NO<sub>2</sub> retrieval algorithm for nadir-viewing satellite instruments:  
18 applications to OMI, *Atmos. Meas. Tech.*, 6, 2607-2626, doi:10.5194/amt-6-2607-2013,  
19 2013.
- 20 Byun, D. W. and Schere, K. L.: Review of the governing equations, computational algorithms,  
21 and other components of the Models-3 Community Multiscale Air Quality (CMAQ)  
22 modeling system overview, *Appl. Mech. Rev.*, 59, 51-77, doi:10.1115/1.2128636, 2006.
- 23 [Chatani, S., Morikawa, T., Nakatsuka, S., Matsunaga, S., and Minoura H.: Development of a](#)  
24 [framework for a high-resolution, three-dimensional regional air quality simulation and its](#)  
25 [application to predicting future air quality over Japan, \*Atmos. Environ.\*, 45, 1383-1393,](#)  
26 [doi:10.1016/j.atmosenv.2010.12.036, 2011.](#)
- 27 Chatani, S. and Sudo, K.: Influences of the variation in inflow to East Asia on surface ozone  
28 over Japan during 1996-2005, *Atmos. Chem. Phys.*, 11, 8745-8758, doi:10.5194/acp-11-  
29 8745-2011, 2011.

- 1 David, L. M. and Nair, P. R.: Diurnal and seasonal variability of surface ozone and NO<sub>x</sub> at a  
2 tropical coastal site: Association with mesoscale and synoptic meteorological conditions,  
3 *J. Geophys. Res.*, 116, D10303, doi:10.1029/2010JD015076, 2011.
- 4 Dee, D. P., Uppala, S. M., Simmons, A. J., Berrisford, P., Poli, P., Kobayashi, S., Andrae, U.,  
5 Balmaseda, M. A., Balsamo, G., Bauer, P., Bechtold, P., Beljaars, A. C. M., van de Berg,  
6 L., Bidlot, J., Bormann, N., Delsol, C., Dragani, R., Fuentes, M., Geer, A. J., Haimberger,  
7 L., Healy, S. B., Hersbach, H., Hólm, E. V., Isaksen, I. S. A., Kållberg, P., Köhler, M.,  
8 Matricardi, M., McNally, A. P., Monge-Sanz, B. M., Morcrette, J.-J., Park, B.-K., Peubey,  
9 C., de Rosnay, P., Tavolato, C., Thépaut, J.-N., and Vitart, F.: The ERA-Interim  
10 reanalysis: configuration and performance of the data assimilation system, *Q. J. Roy.  
11 Meteor. Soc.*, 137, 553-597, doi:10.1002/qj.828, 2011.
- 12 Deeter, M. N., Edwards, D. P., Gille, J. C., Emmons, L. K., Francis, G., Ho, S.-P., Mao, D.,  
13 Masters, D., Worden, H., Drummond, J. R., and Novelli, P. C.: The MOPITT version 4  
14 CO product: algorithm enhancements, validation, and long-term stability, *J. Geophys.  
15 Res.*, 115, D07306, doi:10.1029/2009JD013005, 2010.
- 16 Dentener, F., Stevenson, D., Cofala, J., Mechler, R., Amann, M., Bergamaschi, P., Raes, F.,  
17 and Derwent, R.: The impact of air pollutant and methane emission controls on  
18 tropospheric ozone and radiative forcing: CTM calculations for the period 1990-2030,  
19 *Atmos. Chem. Phys.*, 5, 1731-1755, doi:10.5194/acp-5-1731-2005, 2005.
- 20 Dentener, F., Stevenson, D., Ellingsen, K., van Noije, T., Schultz, M., Amann, M., Atherton,  
21 C., Bell, N., Bergmann, D., Bey, I., Bouwman, L., Butler, T., Cofala, J., Collins, B.,  
22 Drevet, J., Doherty, R., Eickhout, B., Eskes, H., Fiore, A., Gauss, M., Hauglustaine, D.,  
23 Horowitz, L., Isaksen, I. S. A., Josse, B., Lawrence, M., Krol, M., Lamarque, J. F.,  
24 Montanaro, V., Müller, J. F., Peuch, V. H., Pitari, G., Pyle, J., Rast, S., Rodriguez, J.,  
25 Sanderson, M., Savage, N. H., Shindell, D., Strahan, S., Szopa, S., Sudo, K., Van  
26 Dingenen, R., Wild, O., Zeng, G.: The global atmospheric environment for the next  
27 generation, *Environ. Sci. Technol.*, 40, 3586-3594, doi:10.1021/es0523845, 2006.
- 28 Emmons, L. K., Walters, S., Hess, P. G., Lamarque, J.-F., Pfister, G. G., Fillmore, D., Granier,  
29 C., Guenther, A., Kinnison, D., Laepple, T., Orlando, J., Tie, X., Tyndall, G.,  
30 Wiedinmyer, C., Baughcum, S. L., and Kloster, S.: Description and evaluation of the  
31 Model for Ozone and Related chemical Tracers, version 4 (MOZART-4), *Geosci. Model  
32 Dev.*, 3, 43-67, doi:10.5194/gmd-3-43-2010, 2010.

1 European Commission: Joint Research Centre (JRC)/Netherlands Environmental Assessment  
2 Agency (PBL), Emission Database for Global Atmospheric Research (EDGAR), release  
3 version 4.1, available at: <http://edgar.jrc.ec.europa.eu> (last access: 4 October 2013), 2010.

4 Fiore, A. M., West, J. J., Horowitz, L. W., Naik, V., and Schwarzkopf, M. D.: Characterizing  
5 the tropospheric ozone response to methane emission controls and the benefits to climate  
6 and air quality, *J. Geophys. Res.*, 113, D08307, doi:10.1029/2007JD009162, 2008.

7 Fiore, A. M., Naik, V., Spracklen, D. V., Steiner, A., Unger, N., Prather, M., Bergmann, D.,  
8 Cameron-Smith, P. J., Cionni, I., Collins, W. J., Dalsoren, S., Eyring, V., Folberth, G. A.,  
9 Ginoux, P., Horowitz, L. W., Josse, B., Lamarque, J.-F., MacKenzie, I. A., Nagashima, T.,  
10 O'Connor, F. M., Righi, M., Rumbold, S. T., Shindell, D. T., Skeie, R. B., Sudo, K.,  
11 Szopa, S., Takemura, T., and Zeng, G.: Global air quality and climate, *Chem. Soc. Rev.*,  
12 41, 6663-6683, doi:10.1039/c2cs35095e, 2012.

13 Ghude, S. D., Pfister, G. G., Jena, C., van der A, R. J., Emmons, L. K., and Kumar, R.:  
14 Satellite constraints of nitrogen oxide (NO<sub>x</sub>) emissions from India based on OMI  
15 observations and WRF-Chem simulations, *Geophys. Res. Lett.*, 40, 423-428,  
16 doi:10.1029/2012GL053926, 2012.

17 Guenther, A., Karl, T., Harley, P., Wiedinmyer, C., Palmer, P. I., and Geron, C.: Estimates of  
18 global terrestrial isoprene emissions using MEGAN (Model of Emissions of Gases and  
19 Aerosols from Nature), *Atmos. Chem. Phys.*, 6, 3181-3210, doi:10.5194/acp-6-3181-  
20 2006, 2006.

21 Hong Kong Observatory: World Ozone and Ultraviolet Radiation Data Centre (WOUDC)  
22 [Data], available at: <http://www.woudc.org> (last access: 2 July 2012), 2012.

23 IEA: World Energy Outlook 2011, Copernicus Publications, International Energy Agency,  
24 Paris, 2011.

25 IIASA: <http://www.iiasa.ac.at/web/home/research/researchPrograms/Overview2.en.html> (last  
26 access: 23 January 2013), 2013.

27 India Meteorological Department: World Ozone and Ultraviolet Radiation Data Centre  
28 (WOUDC) [Data], available at: <http://www.woudc.org> (last access: 20 November 2013),  
29 2013.

- 1 Itahashi, S., Uno, I., and Kim, S.: Seasonal source contributions of tropospheric ozone over  
2 East Asia based on CMAQ-HDDM, *Atmos. Environ.*, 70, 204-217,  
3 doi:10.1016/j.atmosenv.2013.01.026, 2013.
- 4 JMA: World Ozone and Ultraviolet Radiation Data Centre (WOUDC) [Data], available at:  
5 <http://www.woudc.org> (last access: 2 July 2012), 2012.
- 6 Klimont, Z., Cofala, J., Xing, J., Wei, W., Zhang, C., Wang, S., Kejun, J., Bhandari, P.,  
7 Mathur, R., Purohit, P., Rafaj, P., Chambers, A., and Amann, M.: Projections of SO<sub>2</sub>,  
8 NO<sub>x</sub> and carbonaceous aerosols emissions in Asia, *Tellus B*, 61, 602-617,  
9 doi:10.1111/j.1600-0889.2009.00428.x, 2009.
- 10 Kulkarni, Pavan S., Ghude, Sachin D., and Bortoli, D.: Tropospheric ozone (TOR) trend over  
11 three major inland Indian cities: Delhi, Hyderabad and Bangalore, *Ann. Geophys.*, 28,  
12 1879-1885, doi:10.5194/angeo-28-1879-2010, 2010.
- 13 Kumar, R., Naja, M., Venkataramani, S., and Wild, O.: Variations in surface ozone at  
14 Nainital: A high-altitude site in the central Himalayas, *J. Geophys. Res.*, 115, D16302,  
15 doi:10.1029/2009JD013715, 2010.
- 16 Kumar, R., Naja, M., Pfister, G. G., Barth, M. C., Wiedinmyer, C., and Brasseur, G. P.:  
17 Simulations over South Asia using the Weather Research and Forecasting model with  
18 Chemistry (WRF-Chem): chemistry evaluation and initial results, *Geosci. Model Dev.*, 5,  
19 619-648, doi:10.5194/gmd-5-619-2012, 2012.
- 20 Kurokawa, J., Ohara, T., Uno, I., Hayasaki, M., and Tanimoto, H.: Influence of  
21 meteorological variability on interannual variations of springtime boundary layer ozone  
22 over Japan during 1981-2005, *Atmos. Chem. Phys.*, 9, 6287-6304, doi:10.5194/acp-9-  
23 6287-2009, 2009.
- 24 Lal, S., Naja, M., and Subbaraya, B. H.: Seasonal variations in surface ozone and its  
25 precursors over an urban site in India, *Atmos. Environ.*, 34, 2713-2724,  
26 doi:10.1016/S1352-2310(99)00510-5, 2000.
- 27 Lam, Y. F. and Fu, J. S.: A novel downscaling technique for the linkage of global and  
28 regional air quality modeling, *Atmos. Chem. Phys.*, 9, 9169-9185, doi:10.5194/acp-9-  
29 9169-2009, 2009.

1 Lin, M., Holloway, T., Oki, T., Streets, D. G., and Richter, A.: Multi-scale model analysis of  
2 boundary layer ozone over East Asia, *Atmos. Chem. Phys.*, 9, 3277-3301,  
3 doi:10.5194/acp-9-3277-2009, 2009.

4 Liu, X.-H., Zhang, Y., Xing, J., Zhang, Q., Wang, K., Streets, D. G., Jang, C., Wang, W. X.,  
5 and Hao, J.: Understanding of regional air pollution over China using CMAQ, part II.  
6 Process analysis and sensitivity of ozone and particulate matter to precursor emissions,  
7 *Atmos. Environ.*, 44, 3719-3727, doi:10.1016/j.atmosenv.2010.03.036, 2010.

8 Mauzerall, D. L. and Wang, X. P.: Protecting agricultural crops from the effects of  
9 tropospheric ozone exposure: Reconciling science and standard setting in the United  
10 States, Europe, and Asia, *Annu. Rev. Energ. Env.*, 26, 237-268,  
11 doi:10.1146/annurev.energy.26.1.237, 2001.

12 Naja, M. and Lal, S.: Surface ozone and precursor gases at Gadanki (13.5 degree N, 79.2  
13 degree E), a tropical rural site in India, *J. Geophys. Res.*, D14, 4197,  
14 doi:10.1029/2001JD000357, 2002.

15 Naja, M., Lal, S., and Chand, D.: Diurnal and seasonal variabilities in surface ozone at a high  
16 altitude site Mt Abu (24.6 degree N, 72.7 degree E, 1680 m a.s.l.) in India, *Atmos.*  
17 *Environ.*, 37, 4205-4215, doi:10.1016/S1352-2310(03)00565-X, 2003.

18 NASA Goddard Earth Sciences Data and Information Services Center:  
19 <http://mirador.gsfc.nasa.gov/> (last access: 31 August 2012), 2012.

20 NASA Goddard Space Flight Center: [http://acd-](http://acd-ext.gsfc.nasa.gov/Data_services/cloud_slice/new_data.html)  
21 [ext.gsfc.nasa.gov/Data\\_services/cloud\\_slice/new\\_data.html](http://acd-ext.gsfc.nasa.gov/Data_services/cloud_slice/new_data.html) (last access: 8 October 2012),  
22 2012.

23 NCAR: <http://www.acd.ucar.edu/wrf-chem/mozart.shtml> (last access: 9 April 2013), 2013.

24 Network Center for EANET: Data Report 2010, available at:  
25 <http://www.eanet.asia/product/datarep/datarep10/datarep10.pdf> (last access: 31 May  
26 2012), 2012.

27 Pechony, O., Shindell, D. T., and Faluvegi, G.: Direct top-down estimates of biomass burning  
28 CO emissions using TES and MOPITT vs. bottom-up GFED inventory, *J. Geophys. Res.-*  
29 *Atmos.*, 118, 8054-8066, doi:10.1002/jgrd.50624, 2013.

1 Reddy, B. S. K., Kumar, K. R., Balakrishnaiah, G., Gopal, K. R., Reddy, R. R., Sivakumar, V.,  
2 Lingaswamy, A. P., Arafath, S. M., Umadevi, K., Kumari, S. P., Ahammed, Y. N., and  
3 Lal, S.: Analysis of diurnal and seasonal behavior of surface ozone and its precursors  
4 (NO<sub>x</sub>) at a semi-arid rural site in Southern India, *Aerosol Air Qual. Res.*, 12, 1081-1094,  
5 doi:10.4209/aaqr.2012.03.0055, 2012.

6 Sharma, S., Goel, A., Gupta, D., Kumar, A., Mishra, A., Chatani, S., and Klimont, Z.:  
7 Emission inventory of non-methane volatile organic compounds from anthropogenic  
8 sources in India, in preparation, 2014.

9 Shindell, D., Kuylensstierna, J. C. I., Vignati, E., van Dingenen, R., Amann, M., Klimont, Z.,  
10 Anenberg, S. C., Muller, N., Janssens-Maenhout, G., Raes, F., Schwartz, J., Faluvegi, G.,  
11 Pozzoli, L., Kupiainen, K., Höglund-Isaksson, L., Emberson, L., Streets, D., Ramanathan,  
12 V., Hicks, K., Oanh, N. T. K., Milly, G., Williams, M., Demkine, V., and Fowler, D.:  
13 Simultaneously mitigating near-term climate change and improving human health and  
14 food security, *Science*, 335, 183-189, doi:10.1126/science.1210026, 2012.

15 Sillman, S.: The relation between ozone, NO<sub>x</sub> and hydrocarbons in urban and polluted rural  
16 environments, *Atmos. Environ.*, 33, 1821-1845, doi:10.1016/S1352-2310(98)00345-8,  
17 1999.

18 Skamarock, W. C., Klemp, J. B., Dudhia, J., Gill, D. O., Barker, D. M., Duda, M. G., Huang,  
19 X. Y., Wang, W., and Powers, J. G.: A description of the Advanced Research WRF  
20 Version 3, NCAR/TN-475+STR, 2008.

21 Stevenson, D. S., Young, P. J., Naik, V., Lamarque, J.-F., Shindell, D. T., Voulgarakis, A.,  
22 Skeie, R. B., Dalsoren, S. B., Myhre, G., Berntsen, T. K., Folberth, G. A., Rumbold, S. T.,  
23 Collins, W. J., MacKenzie, I. A., Doherty, R. M., Zeng, G., van Noije, T. P. C., Strunk,  
24 A., Bergmann, D., Cameron-Smith, P., Plummer, D. A., Strode, S. A., Horowitz, L., Lee,  
25 Y. H., Szopa, S., Sudo, K., Nagashima, T., Josse, B., Cionni, I., Righi, M., Eyring, V.,  
26 Conley, A., Bowman, K. W., Wild, O., and Archibald, A.: Tropospheric ozone changes,  
27 radiative forcing and attribution to emissions in the Atmospheric Chemistry and Climate  
28 Model Intercomparison Project (ACCMIP), *Atmos. Chem. Phys.*, 13, 3063-3085,  
29 doi:10.5194/acp-13-3063-2013, 2013.

- 1 Tang, G., Li, X., Wang, Y., Xin, J., and Ren, X.: Surface ozone trend details and  
2 interpretations in Beijing, 2001-2006, *Atmos. Chem. Phys.*, 9, 8813-8823,  
3 doi:10.5194/acp-9-8813-2009, 2009.
- 4 Tanimoto, H.: Increase in springtime tropospheric ozone at a mountainous site in Japan for  
5 the period 1998-2006, *Atmos. Environ.*, 43, 1358-1363,  
6 doi:10.1016/j.atmosenv.2008.12.006, 2009.
- 7 USEPA: <http://www.epa.gov/ttn/chief/software/speciate/index.html> (last access: 23 January  
8 2013), 2013.
- 9 van der Werf, G. R., Randerson, J. T., Giglio, L., Collatz, G. J., Mu, M., Kasibhatla, P. S.,  
10 Morton, D. C., DeFries, R. S., Jin, Y., and van Leeuwen, T. T.: Global fire emissions and  
11 the contribution of deforestation, savanna, forest, agricultural, and peat fires (1997-2009),  
12 *Atmos. Chem. Phys.*, 10, 11707-11735, doi:10.5194/acp-10-11707-2010, 2010.
- 13 Van Vuuren, D. P., Edmonds, J., Kainuma, M., Riahi, K., Thomson, A., Hibbard, K., Hurtt, G.  
14 C., Kram, T., Krey, V., Lamarque, J.-F., Masui, T., Meinshausen, M., Nakicenovic, N.,  
15 Smith, S. J., and Rose, S. K.: The representative concentration pathways: an overview,  
16 *Climatic Change*, 109, 5-31, doi:10.1007/s10584-011-0148-z, 2011.
- 17 Wang, S., Xing, J., Chatani, S., Hao, J., Klimont, Z., Cofala, J., and Amann, M.: Verification  
18 of anthropogenic emissions of China by satellite and ground observations, *Atmos.*  
19 *Environ.*, 45, 6347-6358, doi:10.1016/j.atmosenv.2011.08.054, 2011.
- 20 Wang, T., Wei, X. L., Ding, A. J., Poon, C. N., Lam, K. S., Li, Y. S., Chan, L. Y., and Anson,  
21 M.: Increasing surface ozone concentrations in the background atmosphere of Southern  
22 China, 1994-2007, *Atmos. Chem. Phys.*, 9, 6217-6227, doi:10.5194/acp-9-6217-2009,  
23 2009.
- 24 Wei, W., Wang, S., Chatani, S., Klimont, Z., Cofala, J., and Hao, J.: Emission and speciation  
25 of non-methane volatile organic compounds from anthropogenic sources in China, *Atmos.*  
26 *Environ.*, 42, 4976-4988, doi:10.1016/j.atmosenv.2008.02.044, 2008.
- 27 Whitten, G. Z., Heo, G., Kimura, Y., McDonald-Buller, E., Allen, D. T., Carter, W. P. L., and  
28 Yarwood, G.: A new condensed toluene mechanism for Carbon Bond CB05-TU, *Atmos.*  
29 *Environ.*, 44, 5346-5355, doi:10.1016/j.atmosenv.2009.12.029, 2010.

- 1 WHO: Air Quality Guidelines, Global Update 2005, Particulate Matter, Ozone, Nitrogen  
2 Dioxide and Sulfur Dioxide, WHO Regional Office for Europe, Copenhagen, Denmark,  
3 2006.
- 4 Xing, J., Wang, S. X., Chatani, S., Zhang, C. Y., Wei, W., Hao, J. M., Klimont, Z., Cofala, J.,  
5 and Amann, M.: Projections of air pollutant emissions and its impacts on regional air  
6 quality in China in 2020, *Atmos. Chem. Phys.*, 11, 3119-3136, doi:10.5194/acp-11-3119-  
7 2011, 2011.
- 8 Xu, X., Lin, W., Wang, T., Yan, P., Tang, J., Meng, Z., and Wang, Y.: Long-term trend of  
9 surface ozone at a regional background station in eastern China 1991-2006: enhanced  
10 variability, *Atmos. Chem. Phys.*, 8, 2595-2607, doi:10.5194/acp-8-2595-2008, 2008.
- 11 Yamaji, K., Ohara, T., Uno, I., Kurokawa, J., Pochanart, P., and Akimoto, H.: Future  
12 prediction of surface ozone over east Asia using Models-3 Community Multiscale Air  
13 Quality Modeling System and Regional Emission Inventory in Asia, *J. Geophys. Res.*,  
14 113, D08306, doi:10.1029/2007JD008663, 2008.
- 15 Young, P. J., Archibald, A. T., Bowman, K. W., Lamarque, J.-F., Naik, V., Stevenson, D. S.,  
16 Tilmes, S., Voulgarakis, A., Wild, O., Bergmann, D., Cameron-Smith, P., Cionni, I.,  
17 Collins, W. J., Dalsøren, S. B., Doherty, R. M., Eyring, V., Faluvegi, G., Horowitz, L. W.,  
18 Josse, B., Lee, Y. H., MacKenzie, I. A., Nagashima, T., Plummer, D. A., Righi, M.,  
19 Rumbold, S. T., Skeie, R. B., Shindell, D. T., Strode, S. A., Sudo, K., Szopa, S., and  
20 Zeng, G.: Pre-industrial to end 21st century projections of tropospheric ozone from the  
21 Atmospheric Chemistry and Climate Model Intercomparison Project (ACCMIP), *Atmos.*  
22 *Chem. Phys.*, 13, 2063-2090, doi:10.5194/acp-13-2063-2013, 2013.
- 23 Zhang, Q., Streets, D. G., Carmichael, G. R., He, K. B., Huo, H., Kannari, A., Klimont, Z.,  
24 Park, I. S., Reddy, S., Fu, J. S., Chen, D., Duan, L., Lei, Y., Wang, L. T., and Yao, Z. L.:  
25 Asian emissions in 2006 for the NASA INTEX-B mission, *Atmos. Chem. Phys.*, 9, 5131-  
26 5153, doi:10.5194/acp-9-5131-2009, 2009.
- 27 Zhao, B., Wang, S. X., Dong, X., Wang, J., Duan, L., Fu, X., Hao, J. M., and Fu, J. S.:  
28 Environmental effects of the recent emission changes in China: implications for  
29 particulate matter pollution and soil acidification, *Environ. Res. Lett.*, 8, 024031,  
30 doi:10.1088/1748-9326/8/2/024031, 2013a.

- 1 Zhao, B., Wang, S. X., Wang, J., Fu, J. S., Liu, T., Xu, J., Fu, X., and Hao, J. M.: Impact of  
2 national NO<sub>x</sub> and SO<sub>2</sub> control policies on particulate matter pollution in China, *Atmos.*  
3 *Environ.*, 77, 453-463, doi:10.1016/j.atmosenv.2013.05.012, 2013b.
- 4 Zhao, B., Wang, S. X., Liu, H., Xu, J. Y., Fu, K., Klimont, Z., Hao, J. M., He, K. B., Cofala,  
5 J., and Amann, M.: NO<sub>x</sub> emissions in China: historical trends and future perspectives,  
6 *Atmos. Chem. Phys.*, 13, 9869-9897, doi:10.5194/acp-13-9869-2013, 2013c.
- 7 Ziemke, J. R., Chandra, S., Duncan, B. N., Froidevaux, L., Bhartia, P. K., Levelt, P. F., and  
8 Waters, J. W.: Tropospheric ozone determined from Aura OMI and MLS: evaluation of  
9 measurements and comparison with the Global Modeling Initiative's Chemical Transport  
10 Model, *J. Geophys. Res.*, 111, D19303, doi:10.1029/2006JD007089, 2006.
- 11  
12

1 Table 1. Annual energy consumption and CO<sub>2</sub>, NO<sub>x</sub>, and VOC emissions estimated for 2010  
 2 (BASE) and 2030 under three future scenarios. VOC/NO<sub>x</sub> emission ratios are also shown.

	Country	BASE	BAU0 <sup>1</sup>	PC0 <sup>2</sup>	PC1 <sup>3</sup>
Energy consumption (EJ/year)	China	121.7	199.5	155.0	
	India	26.4	83.8	62.2	
	Japan	21.4	21.5		
	South Korea	10.6	12.2		
	Thailand	5.3	7.7		
	Indonesia	8.2	13.5		
CO <sub>2</sub> emission (Gt/year)	China	8.50	14.10	9.90	
	India	1.71	6.63	4.51	
	Japan	1.25	1.17		
	South Korea	0.63	0.62		
	Thailand	0.28	0.44		
	Indonesia	0.43	0.81		
NO <sub>x</sub> emission (Mt/year)	China	26.1	35.4	25.2	11.5
	India	5.6	19.5	13.4	6.8
	Japan	1.70	0.86		
	South Korea	1.18	0.84		
	Thailand	0.86	1.16		
	Indonesia	1.58	1.88		
VOC emission (Mt/year)	China	22.8	29.0	24.4	16.8
	India	10.2	19.8	16.0	11.4
	Japan	1.41	1.11		
	South Korea	0.67	0.51		
	Thailand	0.91	0.81		
	Indonesia	3.98	3.68		
VOC/NO <sub>x</sub> emission ratio	China	0.87	0.82	0.97	1.47
	India	1.82	1.02	1.19	1.68
	Japan	0.83	1.29		
	South Korea	0.57	0.61		
	Thailand	1.06	0.70		
	Indonesia	2.52	1.96		

1 <sup>1</sup> BAU0 scenario is based on current legislations and implementation status for energy saving  
2 policies and end-of-pipe control strategies.

3 <sup>2</sup> PC0 scenario assumes that new energy-saving policies will be released and enforced more  
4 stringently. End-of-pipe control strategies are the same as BAU0.

5 <sup>3</sup> PC1 scenario assumes that new pollution control policies would be released and  
6 implemented. Energy-saving policies are the same as PC0.

7

8

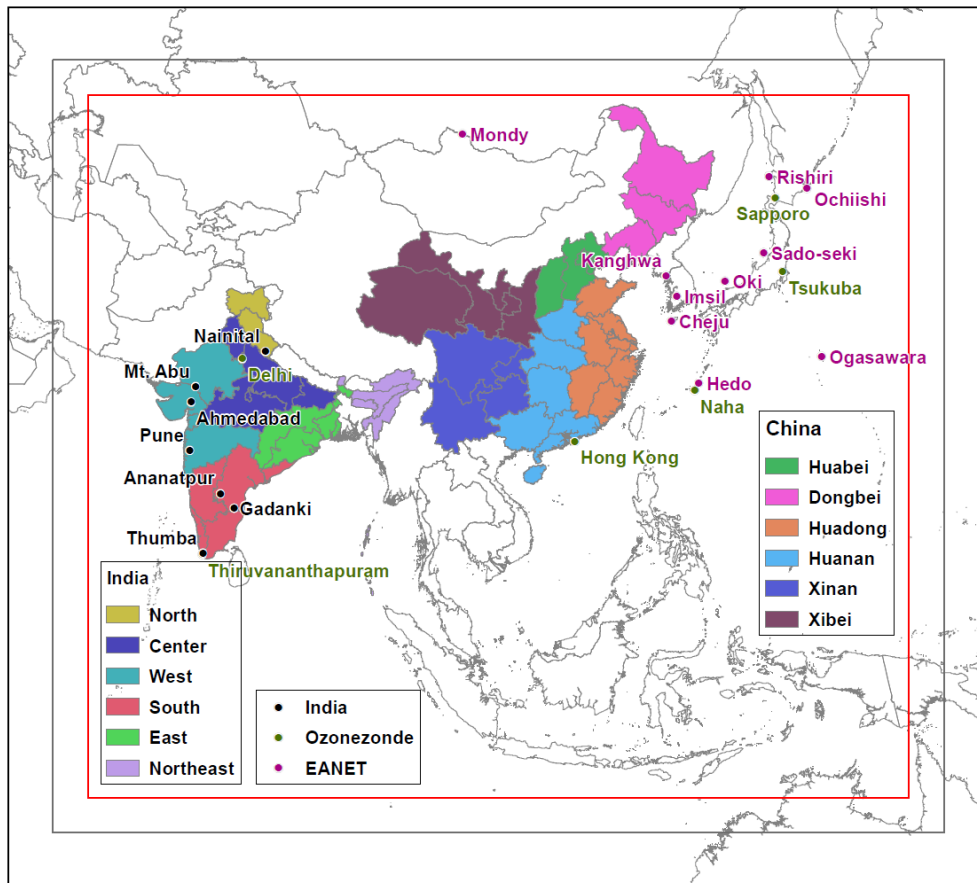
1 Table 2 Overview of simulation cases performed in this study.

2

Case	Emission	Other change
BASE	BASE	
BAU0nox	BAU0 (NOx only) + BASE	
BAU0voc	BAU0 (VOC only) + BASE	
BAU0	BAU0	
BAU0o3	BAU0	+ 5ppb boundary ozone
BAU0ch4	BAU0	+ 400ppb background methane
BAU0ta	BAU0	- 5degC temperature
PC0	PC0	
PC1	PC1	

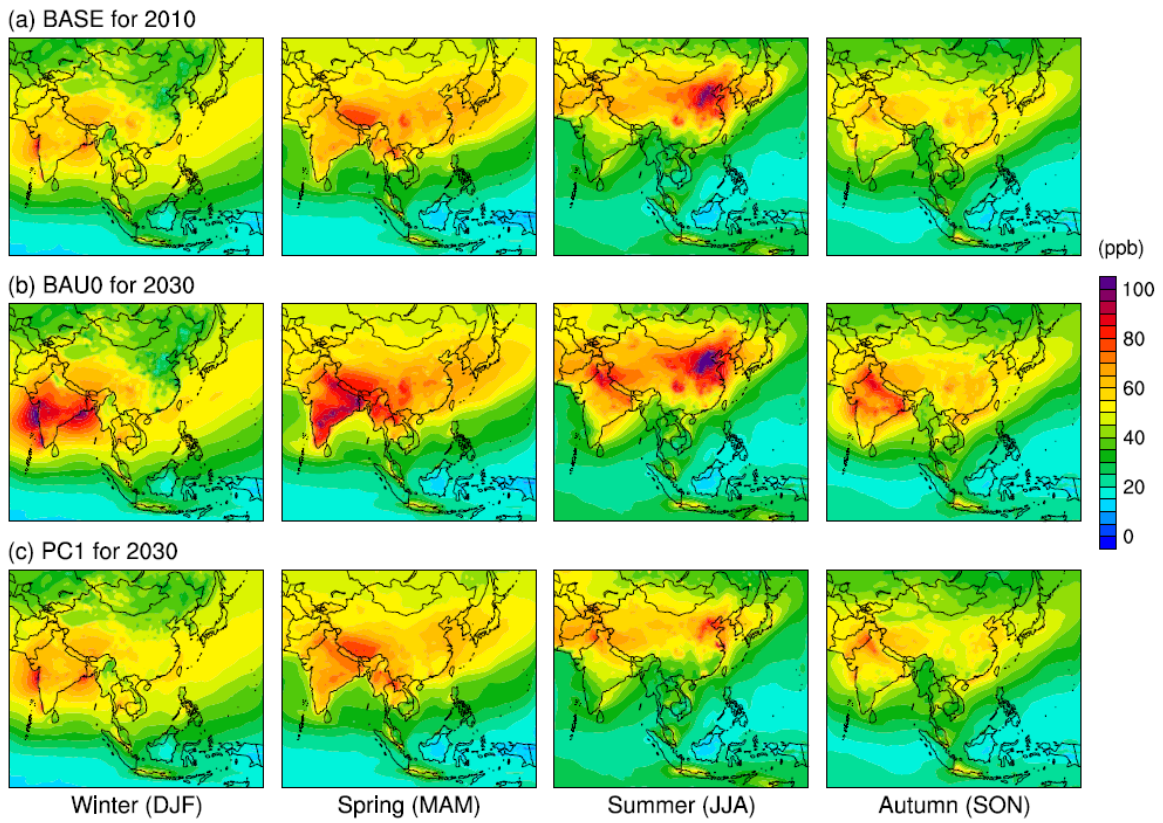
3

4



1  
2  
3  
4  
5  
6

Fig. 1. Target domains of WRF-ARW (gray) and CMAQ (red). Monitoring sites of EANET, ozonezone, and India are indicated. Regions in China and India are color-coded.



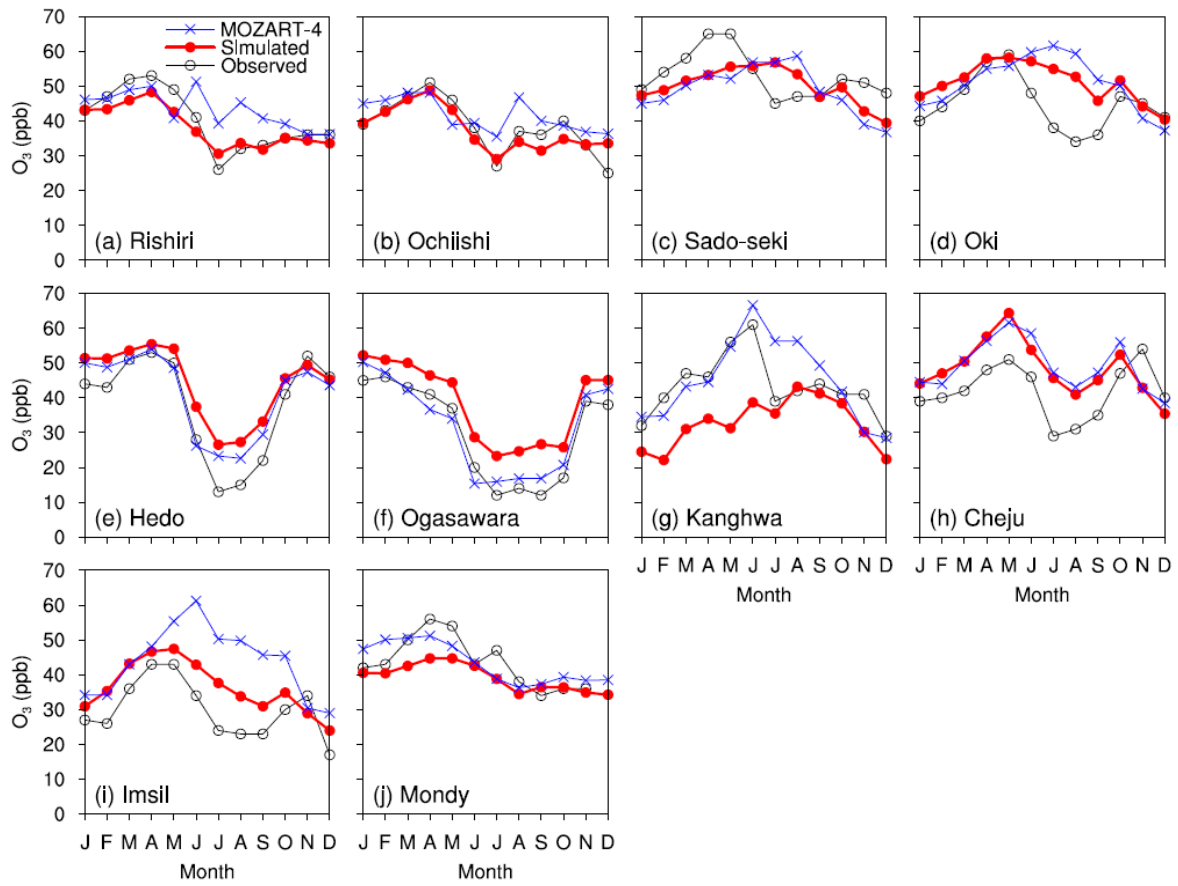
1

2 Fig. 2. Horizontal distributions of simulated seasonal mean surface ozone concentration in (a)

3 BASE for 2010, (b) BAU0 for 2030, and (c) PC1 for 2030.

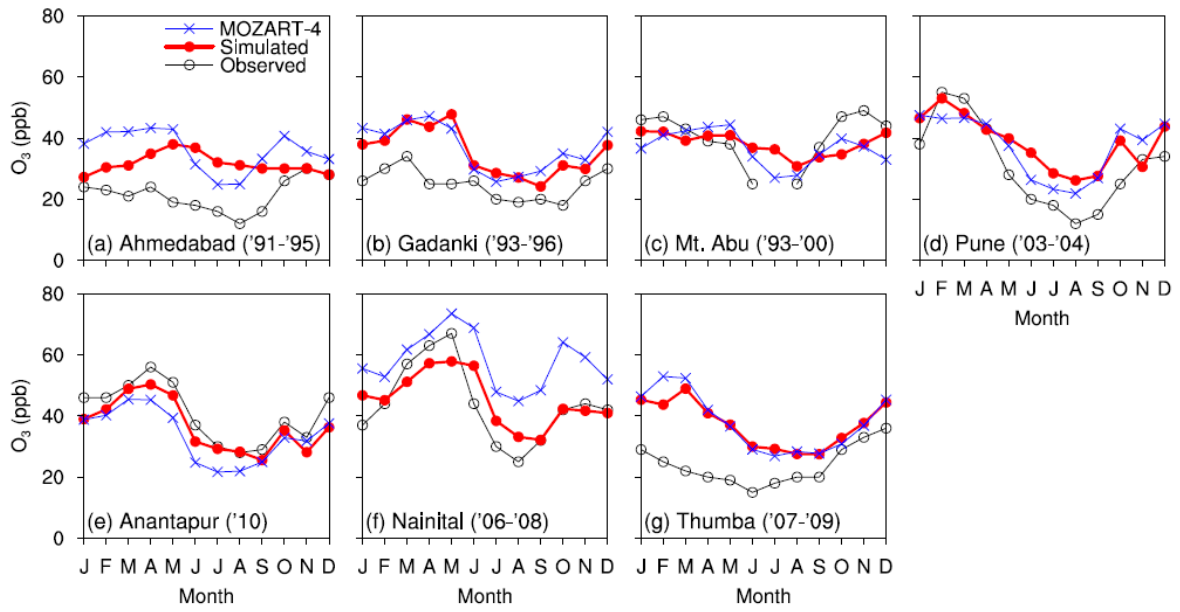
4

5



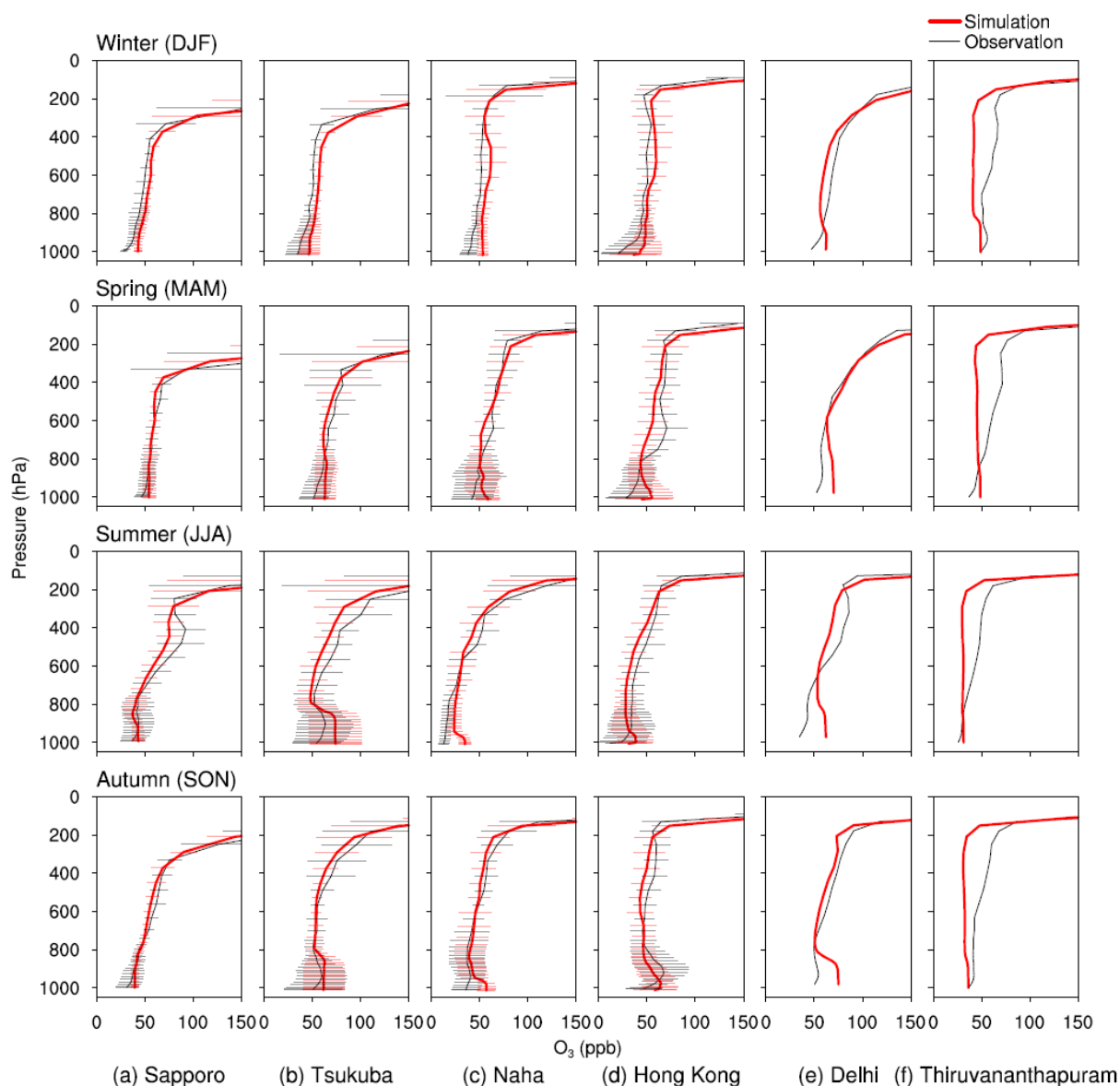
1  
2  
3  
4  
5  
6

Fig. 3. Monthly mean observed and simulated surface ozone concentration in BASE for 2010 at ten EANET monitoring sites. Results of MOZART-4 are also shown.



1  
2  
3  
4  
5  
6  
7

Fig. 4. Monthly mean observed and simulated surface ozone concentration in BASE for 2010 at seven sites in India. Results of MOZART-4 are also shown. Target years of observations are shown along site names.



1  
2  
3  
4  
5  
6  
7  
8  
9  
10

Fig. 5. Vertical profiles of observed and simulated ozone concentration in BASE for 2010 at six monitoring stations. Values are averaged over all ozonesonde measurements within each season at Sapporo, Tsukuba, Naha, and Hong Kong. Error bars represent standard deviations. Simulated seasonal mean values are compared with values averaged over all available ozonesonde measurements within each season during 2000-2011 at Delhi and Thiruvananthapuram.

1

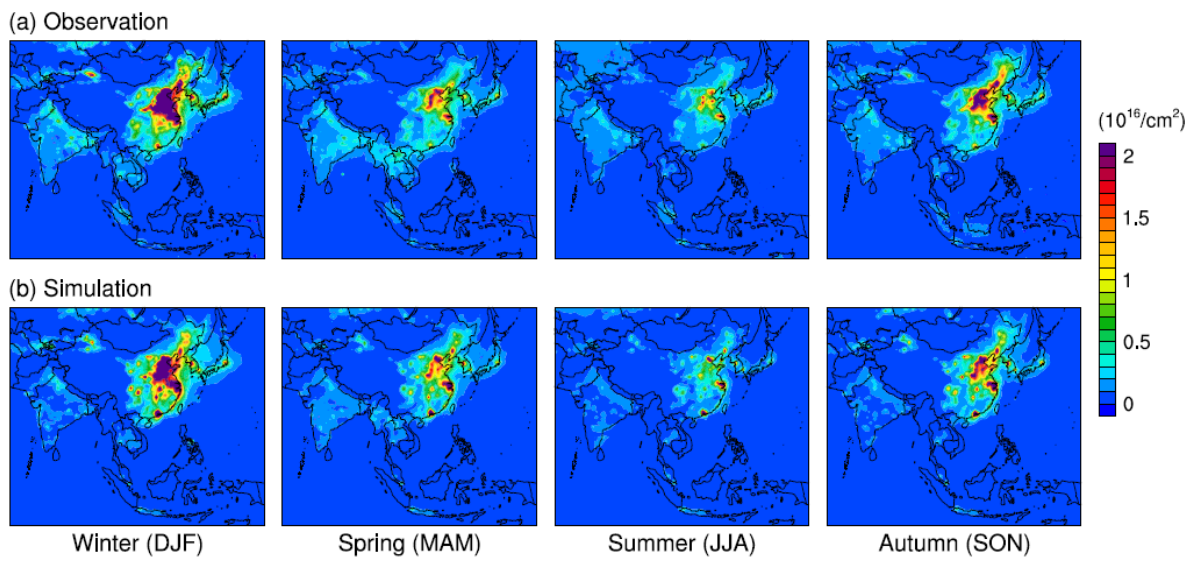
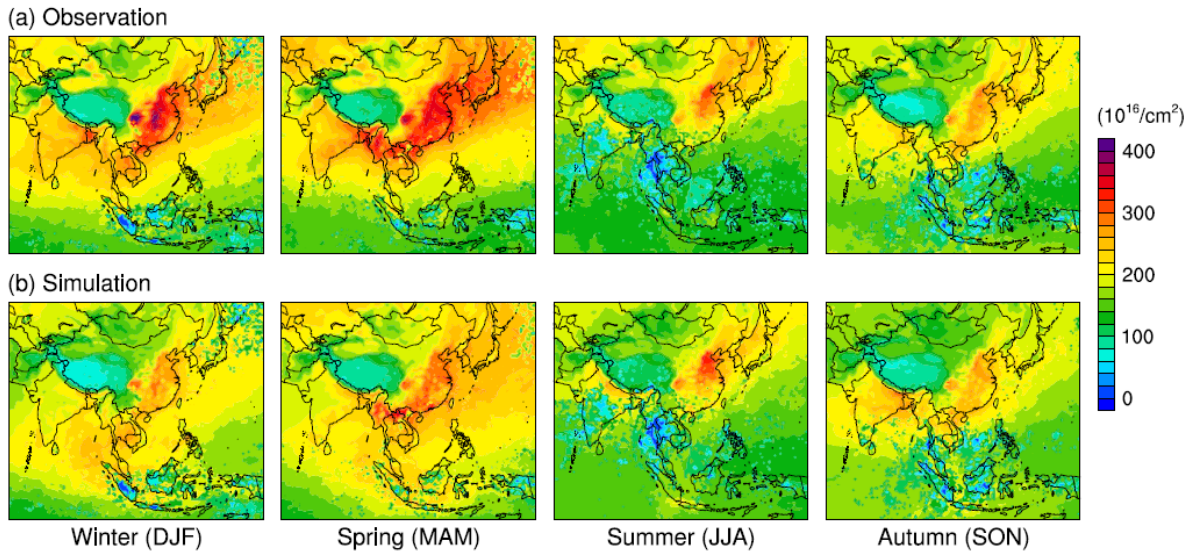


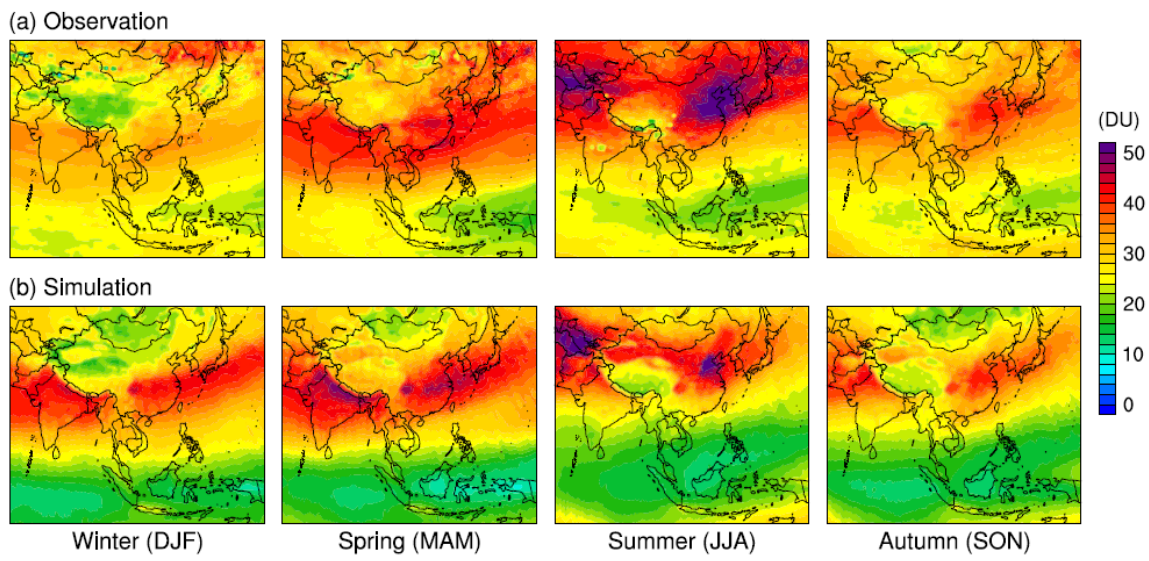
Fig. 6. Horizontal distributions of observed and simulated seasonal mean tropospheric column NO<sub>2</sub> in BASE for 2010.



1  
2  
3  
4  
5  
6

Fig. 7. Horizontal distributions of observed and simulated seasonal mean total column CO in BASE for 2010.

1



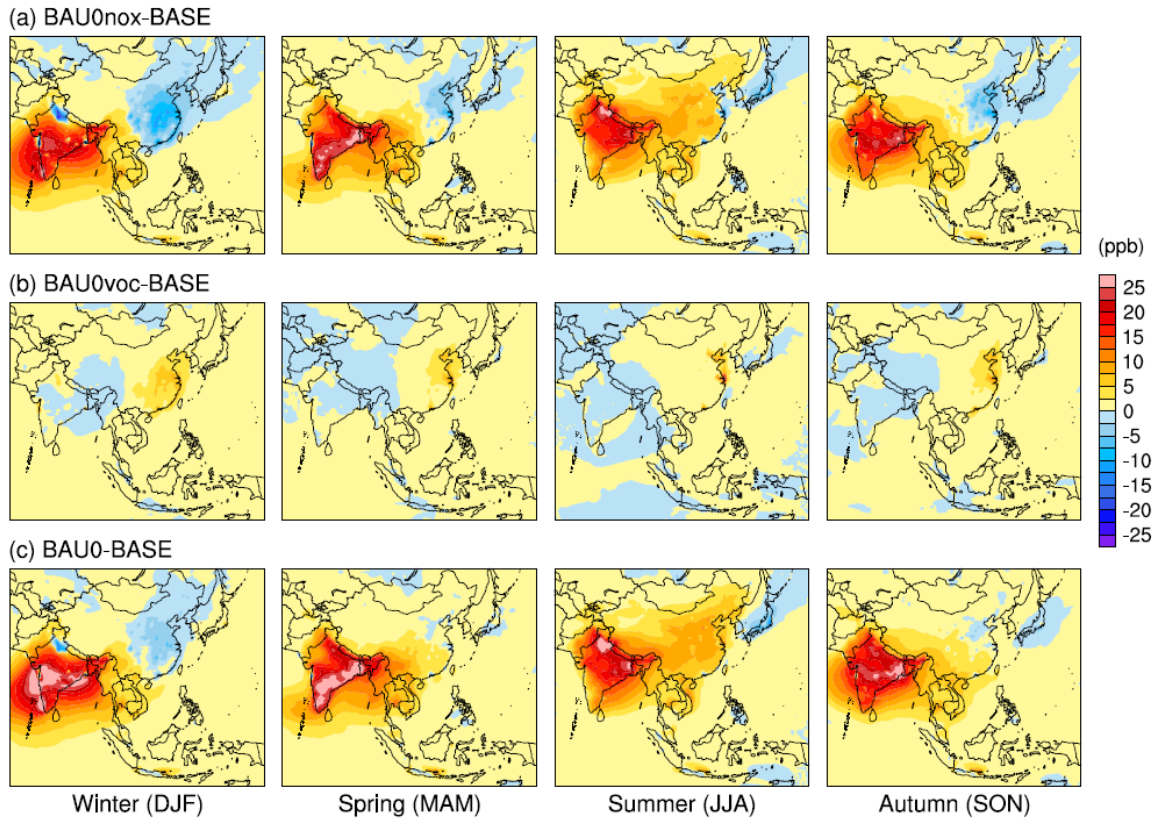
2

3

4 Fig. 8. Horizontal distributions of observed and simulated seasonal mean tropospheric  
5 column ozone in BASE for 2010.

6

7



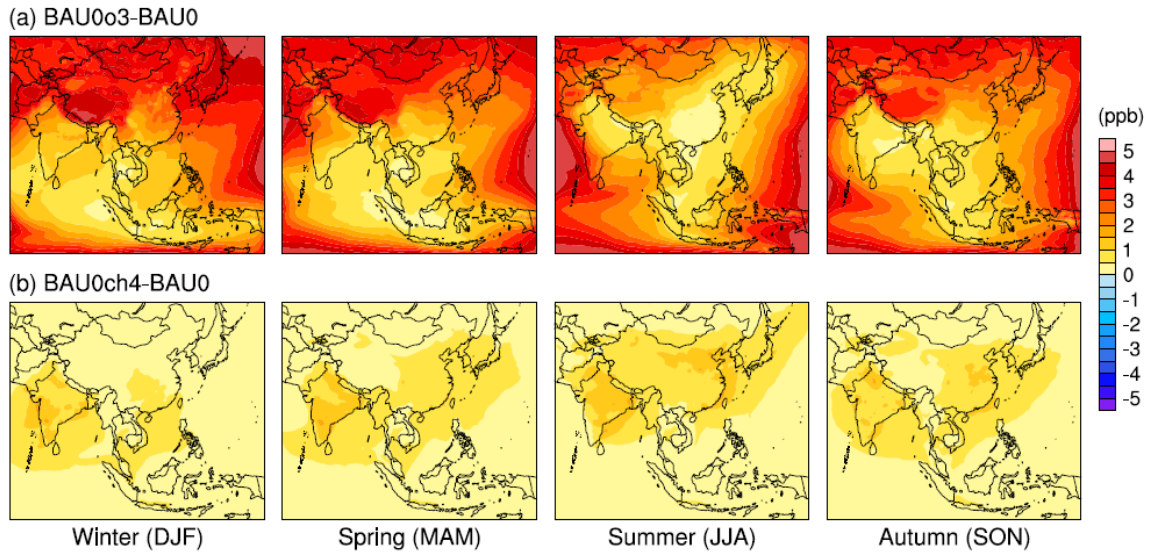
1

2

3 Fig. 9. Horizontal distributions of differences in simulated seasonal mean surface ozone  
 4 concentrations between (a) BAU0nox and BASE, (b) BAU0voc and BASE, and (c) BAU0  
 5 and BASE.

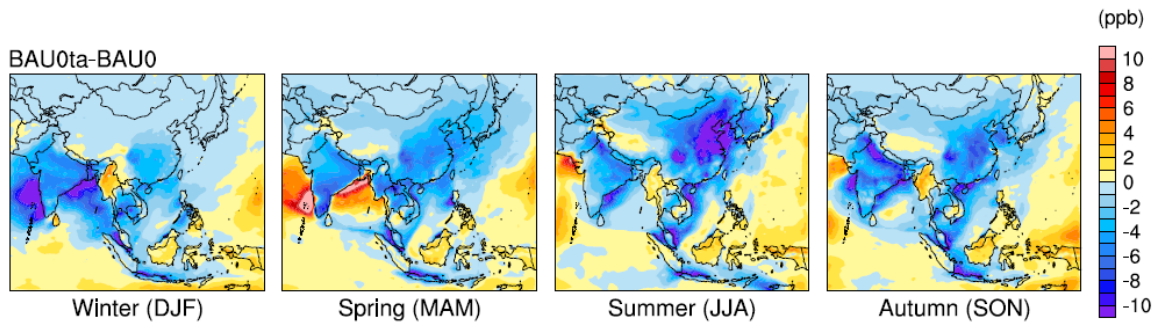
6

7



1  
2  
3  
4  
5  
6

Fig. 10. Horizontal distributions of differences in simulated seasonal mean surface ozone concentrations between (a) BAU0o3 and BAU0, and (b) BAU0ch4 and BAU0.



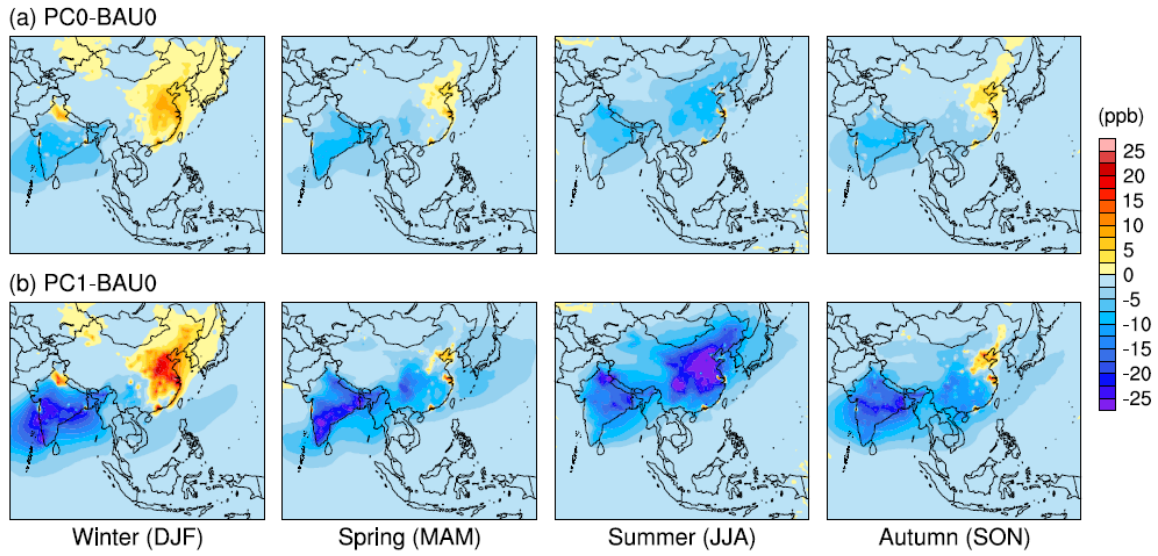
1

2

3 Fig. 11. Horizontal distributions of differences in simulated seasonal mean surface ozone  
4 concentrations between BAU0ta and BAU0.

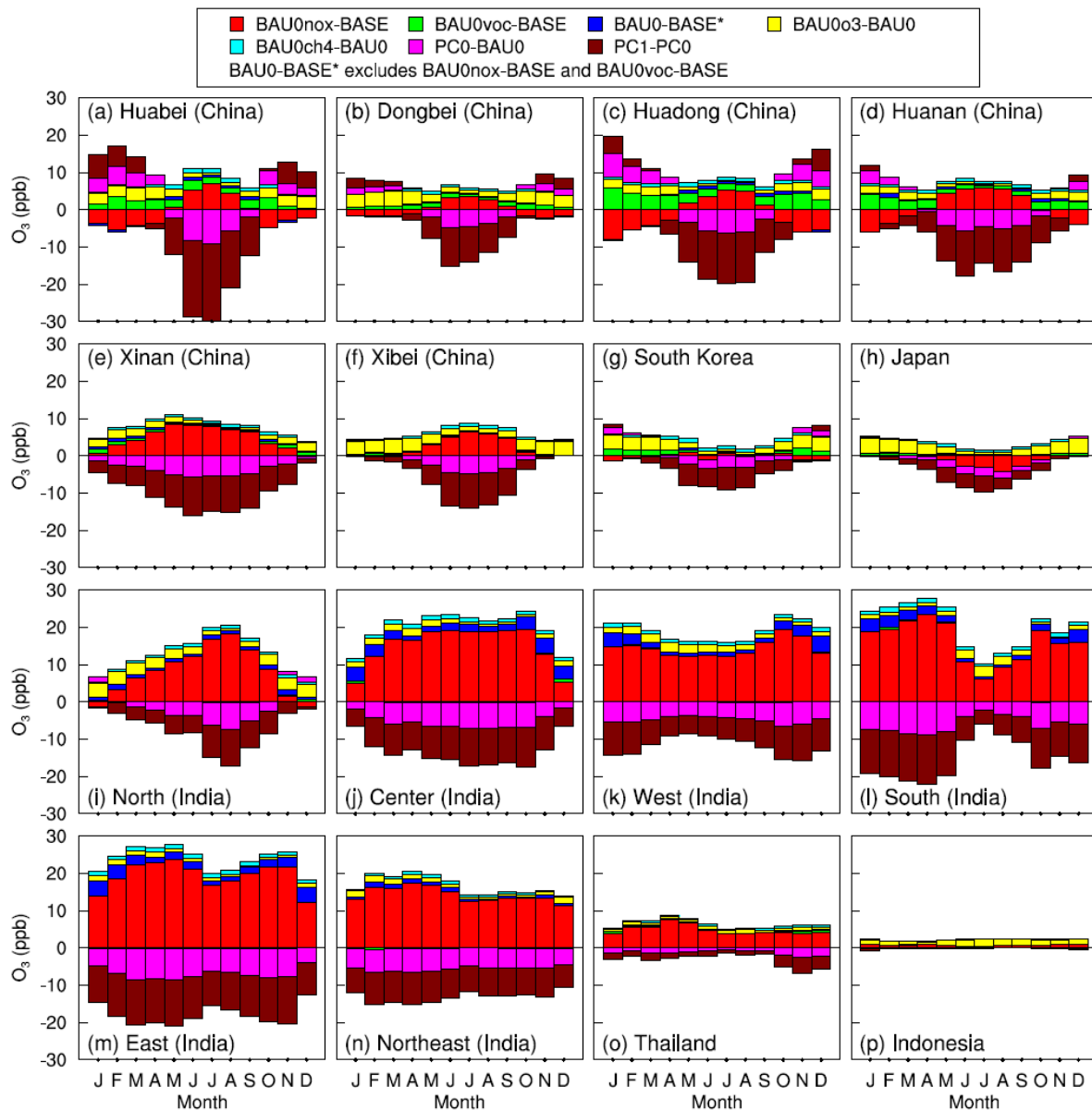
5

6



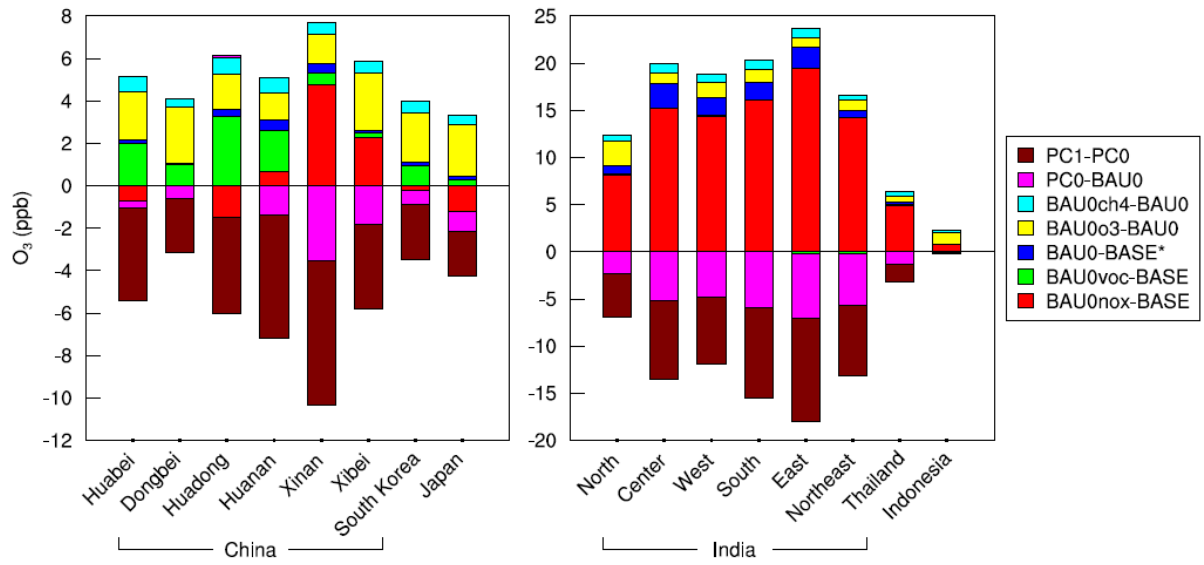
1  
2  
3  
4  
5  
6

Fig. 12. Horizontal distributions of differences in simulated seasonal mean surface ozone concentrations between (a) PC0 and BAU0, and (b) PC1 and BAU0.



1  
2  
3  
4  
5  
6  
7

Fig. 13 Differences in simulated monthly mean surface ozone concentrations among cases which are averaged over regions in China and India as well as Japan, South Korea, Thailand, and Indonesia.



1  
2  
3  
4  
5  
6

Fig. 14 Differences in simulated annual mean surface ozone concentrations among cases which are averaged over regions in China and India as well as Japan, South Korea, Thailand, and Indonesia.